



Tracking eolian dust with helium and thorium: Impacts of grain size and provenance

David McGee^{a,*}, Gisela Winckler^{b,c}, Alejandra Borunda^{b,c}, Sascha Serno^{b,d,1},
Robert F. Anderson^{b,c}, Cristina Recasens^b, Aloys Bory^e, Diego Gaiero^f,
Samuel L. Jaccard^g, Michael Kaplan^b, Jerry F. McManus^{b,c}, Marie Revel^h,
Youbin Sunⁱ

^a Department of Earth, Atmospheric and Planetary Sciences, Massachusetts Institute of Technology, Cambridge, MA, USA

^b Lamont-Doherty Earth Observatory, Columbia University, Palisades, NY, USA

^c Department of Earth and Environmental Sciences, Columbia University, New York, NY, USA

^d DFG-Leibniz Center for Earth Surface Processes and Climate Studies, University of Potsdam, Potsdam, Germany

^e Univ. Lille, CNRS, Univ. Littoral Côte d'Opale, UMR 8187, LOG, Laboratoire d'Océanologie et de Géosciences, F 59 000 Lille, France

^f Centro de Investigaciones en Ciencias de la Tierra (CICTERRA-CONICET), FCEfyN, Universidad Nacional de Córdoba, Córdoba, Argentina

^g Institute of Geological Sciences and Oeschger Center for Climate Change Research, University of Bern, Bern, Switzerland

^h Geoazur, 250 Rue Albert Einstein, 06560 Valbonne-Sophia Antipolis, France

ⁱ State Key Laboratory of Loess and Quaternary Geology, Institute of Earth Environment, Chinese Academy of Sciences, Xi'an, China

Received 28 April 2015; accepted in revised form 16 November 2015; available online 29 November 2015

Abstract

Reconstructions of the deposition rate of windblown mineral dust in ocean sediments offer an important means of tracking past climate changes and of assessing the radiative and biogeochemical impacts of dust in past climates. Dust flux estimates in ocean sediments have commonly been based on the operationally defined lithogenic fraction of sediment samples. More recently, dust fluxes have been estimated from measurements of helium and thorium, as rare isotopes of these elements (He-3 and Th-230) allow estimates of sediment flux, and the dominant isotopes (He-4 and Th-232) are uniquely associated with the lithogenic fraction of marine sediments. In order to improve the fidelity of dust flux reconstructions based on He and Th, we present a survey of He and Th concentrations in sediments from dust source areas in East Asia, Australia and South America. Our data show systematic relationships between He and Th concentrations and grain size, with He concentrations decreasing and Th concentrations increasing with decreasing grain size. We find consistent He and Th concentrations in the fine fraction (<5 μm) of samples from East Asia, Australia and Central South America (Puna-Central West Argentina), with Th concentrations averaging 14 μg/g and He concentrations averaging 2 μcc STP/g. We recommend use of these values for estimating dust fluxes in sediments where dust is dominantly fine-grained, and suggest that previous studies may have systematically overestimated Th-based dust fluxes by 30%. Source areas in Patagonia appear to have lower He and Th contents than other regions, as fine fraction concentrations average 0.8 μcc STP/g and 9 μg/g for ⁴He and ²³²Th, respectively. The impact of grain size on lithogenic He and Th concentrations should be taken into account in sediments proximal to dust sources where dust grain size may vary considerably. Our data also have important implications for the hosts of He in long-traveled dust and for the ³He/⁴He ratio used for terrigenous He in studies of extraterrestrial He in sediments and ice.

We also investigate the use of He/Th ratios as a provenance tracer. Our results suggest differences in fine fraction He/Th ratios between East Asia, Australia, central South America and Patagonia, with ratios showing a positive relationship with

* Corresponding author. Tel.: +1 617 324 3545; fax: +1 617 253 8630.

E-mail address: davidmccg@mit.edu (D. McGee).

¹ Present address: School of GeoSciences, University of Edinburgh, Edinburgh, UK.

the geological age of source rocks. He/Th ratios may thus provide useful provenance information, for example allowing separation of Patagonian sources from Puna-Central West Argentina or Australian dust sources. He/Th ratios in open-ocean marine sediments are similar to ratios in the fine fraction of upwind dust source areas. He/Th ratios in mid-latitude South Atlantic sediments suggest that dust in this region primarily derives from the Puna-Central West Argentina region (23–32° S) rather than Patagonia (>38°S). In the equatorial Pacific, He/Th ratios are much lower than in extratropical Pacific sediments or potential source areas measured as a part of this study (East Asia, South America, Australia) for reasons that are at present unclear, complicating their use as provenance tracers in this region.

© 2015 Elsevier Ltd. All rights reserved.

1. INTRODUCTION

Records of eolian mineral dust flux and provenance preserved in ocean sediments, ice cores and terrestrial deposits offer essential insights into past climates. Past dust fluxes provide information about aridity (Rea, 1994; deMenocal et al., 2000) and sediment supply (Sugden et al., 2009) in dust source areas as well as about the strength of winds responsible for dust entrainment and transport (McGee et al., 2010a). Dust provides limiting micronutrients, especially iron, to the surface ocean and to nutrient-depleted soils (Okin et al., 2004; Jickells et al., 2005); it also impacts the Earth's radiative balance, affecting both surface temperatures and precipitation (Miller et al., 2004). Accurate dust flux reconstructions are required to estimate the importance of these effects as drivers of past climate and biogeochemical changes (e.g., Claquin et al., 2003; Martínez-García et al., 2014).

Reconstructions from terrestrial settings such as loess deposits (e.g., Kohfeld and Harrison, 2003; Sun and An, 2005; Bettis et al., 2003), peat bogs (e.g., Weiss et al., 2002; Kylander et al., 2007; Ferrat et al., 2011; Sharifi et al., 2015) and lakes (e.g., Yancheva et al., 2007; Neff et al., 2008) provide important information about dust emissions and transport close to the source, while dust flux records from polar ice cores offer insights into long-range transport (e.g., Biscaye et al., 1997; Fischer et al., 2007). Records from marine sediments fill the middle ground between these archives, offering broad spatial and temporal coverage as well as direct insights into relationships between dust deposition and marine biogeochemistry. Here we focus on improving dust flux reconstructions from marine sediments, though the data presented have applications in terrestrial sedimentary and ice archives as well.

Dust flux reconstructions from marine sediments require an accurate estimate of the concentration of windblown dust in the sediment. In the past decade, several studies have used the dominant isotopes of helium and thorium, ^4He and ^{232}Th , to infer dust concentrations in sediments (e.g., Patterson et al., 1999; Marcantonio et al., 2001a, 2009; Anderson et al., 2006; McGee et al., 2007; Winckler et al., 2008; Serno et al., 2014, 2015). Both isotopes are highly enriched in lithogenic minerals relative to marine biogenic sediments, and they are less susceptible to contamination by volcanic inputs than other markers of lithogenic inputs (e.g., Al, Ti). In sediments in which non-volcanic

lithogenic inputs are dominantly eolian, ^4He and ^{232}Th can thus provide estimates of eolian dust concentrations. An additional reason for their use is convenience: ^4He and ^{232}Th are measured as a part of routine analysis for the minor isotopes ^3He and ^{230}Th , respectively, both of which are used for determining accumulation rates in marine sediments (Francois et al., 2004; McGee and Mukhopadhyay, 2013).

In settings in which ^4He or ^{232}Th are dominantly derived from eolian dust, both dust concentration and bulk sediment flux can then be derived from a single analysis, allowing calculation of the dust flux (Marcantonio et al., 2001a, 2009; Winckler et al., 2005, 2008; Anderson et al., 2006; McGee et al., 2007; Serno et al., 2014) using the following equation:

$$F_{dust} = \frac{[X]_{sed} \cdot MAR}{[X]_{dust}} \quad (1)$$

where F_{dust} is dust flux, MAR is the mass accumulation rate (or flux) of the sediment (derived from ^3He or ^{230}Th data), $[X]_{sed}$ is the ^4He or ^{232}Th concentration measured in the sediment and $[X]_{dust}$ is the ^4He or ^{232}Th concentration assumed for eolian dust. Converting from ^4He and ^{232}Th concentrations to dust concentrations and fluxes thus requires an accurate estimate of ^4He and ^{232}Th concentrations in dust. At present, we have a limited understanding of the mean values and variability of these concentrations between source areas or grain size fractions.

Constraints on dust provenance are essential to the interpretation of dust flux records. Knowledge of dust provenance links downwind fluxes to source area conditions and atmospheric circulation patterns. Provenance information also helps constrain dust's past climate impacts, as radiative properties and iron availability differ significantly among dust source areas (Sokolik and Toon, 1999; Dubovik et al., 2002; Schroth et al., 2009). A wide variety of dust provenance tracers exists, including mineralogy (Blank et al., 1985), radiogenic isotopes (Grousset and Biscaye, 2005), trace element ratios (Ferrat et al., 2011; Pourmand et al., 2014), and electron spin resonance signal intensity and crystallinity index of quartz (Sun et al., 2013). Despite this large number of tools, dust provenance in distal regions such as the equatorial Pacific, high-latitude oceans and polar ice sheets remains poorly constrained, in part because of significant overlap in dust source area compositions in common provenance measurements. It has

been suggested that $^4\text{He}/^{232}\text{Th}$ ratios may offer valuable dust provenance information (Winckler et al., 2008; Woodard et al., 2012; Serno et al., 2014), but little is known about controls on $^4\text{He}/^{232}\text{Th}$ ratios in dust.

Here we provide a suite of measurements of ^4He and ^{232}Th concentrations and $^4\text{He}/^{232}\text{Th}$ ratios in ocean sediments and samples from dust source areas in East Asia, Australia, and South America. We examine variations in these measures both between dust source areas and in different grain size fractions. These measurements provide insights into the use of ^4He and ^{232}Th as dust proxies and the potential use of $^4\text{He}/^{232}\text{Th}$ as a dust provenance indicator.

1.1. ^4He as a dust proxy

^4He has been used as a dust proxy in a variety of settings. It was first used in marine sediments ranging in age from the Quaternary (Patterson et al., 1999; Winckler et al., 2005, 2008; Serno et al., 2014, 2015) to the early Cenozoic (Marcantonio et al., 2009), and more recently it has been employed as a dust tracer in Antarctic ice (Winckler and Fischer, 2006) and corals (Mukhopadhyay and Kreycik, 2008). Additionally, $^4\text{He}/\text{Ca}$ ratios have been interpreted as a dust provenance tracer in Antarctic ice (Winckler and Fischer, 2006). The minor isotope of He, ^3He , is commonly measured to calculate the concentration of extraterrestrial ^3He ($^3\text{He}_{\text{ET}}$) in sediments, from which sediment accumulation rates can be estimated (Marcantonio et al., 1995; McGee and Mukhopadhyay, 2013); ^3He and ^4He concentrations are obtained during the same measurement.

^4He in continental sediments such as dust dominantly reflects alpha particles from U and Th decay (Rutherford, 1905; Patterson et al., 1999). Recent volcanics may contain mantle-derived He, but typical concentrations are only $\sim 10^{-2}$ $\mu\text{cc STP/g}$, roughly two to three orders of magnitude lower than He concentrations in typical continental sediments (Mamyrin and Tolstikhin, 1984; Farley, 2001; Kurz et al., 2004). Submarine volcanic glasses may contain He concentrations of ~ 1 $\mu\text{cc STP/g}$ (Graham et al., 1992), as degassing is reduced by the pressure of overlying water, but these glasses are not thought to disperse significant distances from mid-ocean ridges and ocean island volcanoes. As an inert gas, He is not associated with biogenic or authigenic phases in marine sediments (Patterson et al., 1999; Mukhopadhyay and Kreycik, 2008).

^4He concentrations in dust potentially reflect a variety of factors governing ^4He production and loss. ^4He production is a function of the U and Th content and age of source rocks, while ^4He loss reflects the He retentivity of minerals in the dust source area, which may be determined both by primary source rock mineralogy and subsequent weathering. ^4He concentrations vary widely among different minerals as a result of differences in U and Th concentrations and He retentivity. For example, zircon and uraninite commonly have He concentrations on the order of 10^4 $\mu\text{cc STP/g}$, while concentrations in coarse quartz and feldspar grains are on the order of 1 $\mu\text{cc STP/g}$ (Mamyrin and Tolstikhin, 1984; Martel et al., 1990). Once grains have

been weathered to grain sizes typical of long-traveled dust (≤ 5 μm) (Tsoar and Pye, 1987; Rea and Hovan, 1995), they do not accumulate further ^4He from U and Th decay, as the recoil length of alpha particles is 10–30 μm (Farley, 1995; Ballentine and Burnard, 2002).

^4He concentrations in global dust sources are poorly known, as is the behavior of ^4He -rich grains during the sorting that accompanies dust entrainment, transport and deposition. ^4He flux records thus are interpreted as reflecting relative changes in dust flux but are not typically used to quantify dust deposition unless a local calibration is determined (e.g., Mukhopadhyay and Kreycik, 2008).

1.2. ^{232}Th as a dust proxy

^{232}Th has received increasing use as a dust proxy in marine sediments in recent years, including studies in the northern tropical Atlantic (Adkins et al., 2006), equatorial Atlantic (Bradtmiller et al., 2007), Arabian Sea (Marcantonio et al., 2001a; Pourmand et al., 2004), equatorial Pacific (Anderson et al., 2006; McGee et al., 2007; Winckler et al., 2008), North Pacific (Woodard et al., 2012; Serno et al., 2014) and Southern Ocean (Martínez-García et al., 2009; Lamy et al., 2014). Conveniently, a minor isotope of Th, ^{230}Th , is commonly used to calculate sediment fluxes (Francois et al., 2004), and ^{232}Th data are collected as a part of routine analysis for excess ^{230}Th . Measurements of $^{232}\text{Th}/^{230}\text{Th}$ in seawater have also emerged as a promising tracer of modern eolian dust deposition in the ocean (Hsieh et al., 2011; Hayes et al., 2013).

A survey of published results from <63 μm sediments found that ^{232}Th concentrations are relatively uniform in global dust sources (McGee et al., 2007), with most values falling within ~ 2 ppm of the upper continental crustal average of 10.7 ppm (Taylor and McLennan, 1985). ^{232}Th concentrations are typically 1–2 orders of magnitude lower in mafic volcanic rocks, the dominant lithology produced by mid-ocean ridge and ocean island volcanism (Taylor and McLennan, 1985; Olivarez et al., 1991); contamination of marine ^{232}Th fluxes by mafic detritus is thus unlikely. ^{232}Th concentrations in continental arcs and some island arcs are similar to those in continental sediments, so silicic ashes may contribute significantly to sedimentary ^{232}Th inventories. As with He, hemipelagic material and ice-rafted detritus are additional potential contaminants. ^{232}Th is not associated with biogenic sediments (Woodard et al., 2012).

Several studies have attempted to determine the fraction of dust-derived Th that dissolves in the upper water column, with estimates ranging from 1% to 20% (Arraes-Mescoff et al., 2001; Roy-Barman et al., 2002; Hsieh et al., 2011; Hayes et al., 2013). The most recent studies favor the higher end of this range (Hayes et al., 2013). This dissolved fraction has a short (decades) residence time in the open ocean water column (Moore and Sackett, 1964; Anderson et al., 1983), meaning that the potential for lateral transport of dissolved Th is limited. Because Th solubility and residence time are small but non-zero, total (scavenged + particulate) ^{232}Th fluxes measured in the sediment may reflect some degree of homogenization by

advection and diffusion in the overlying water column and thus represent a regionally averaged dust flux.

1.3. $^4\text{He}/^{232}\text{Th}$ ratios as indicators of dust provenance

Winckler et al. (2008) found that $^4\text{He}/^{232}\text{Th}$ ratios in 3 cores spanning the breadth of the equatorial Pacific were approximately constant over the past several glacial–interglacial cycles. This study found that $^4\text{He}/^{232}\text{Th}$ ratios were not significantly different in cores from the western and central equatorial Pacific (ODP806C, TT013-PC72; see Table EA2 for locations), and that $^4\text{He}/^{232}\text{Th}$ ratios were lower in the core from the eastern equatorial Pacific (ODP849). Winckler et al. (2008) interpreted these results as reflecting differences in the age distribution of bedrock in dust source areas, consistent with observational and provenance data suggesting that the eastern equatorial Pacific receives dust from young, presumably ^4He -poor dust sources in North and South America (Stancin et al., 2006; Xie and Marcantonio, 2012; Pichat et al., 2014), while the central and western equatorial Pacific receives dust from older Asian sources (Merrill et al., 1989; Stancin et al., 2006). Woodard et al. (2012) found that $^4\text{He}/^{232}\text{Th}$ ratios in Shatsky Rise sediments deposited in the equatorial Pacific in the late Paleocene (58 Ma) were higher than the late Pleistocene results of Winckler et al. (2008). These authors also interpreted $^4\text{He}/^{232}\text{Th}$ ratios in terms of the mean age of source rocks, suggesting that dust transported to the Paleocene equatorial Pacific may have derived from sources with a greater mean age. Finally, Serno et al. (2014) found that $^4\text{He}/^{232}\text{Th}$ ratios of Holocene sediments in open ocean sites in the North Pacific were similar to $^4\text{He}/^{232}\text{Th}$ ratios in $<8\ \mu\text{m}$ sediments from East Asian dust source areas, but substantially higher than either the late Pleistocene or Paleocene equatorial Pacific sediments. This study suggested that there may be substantial changes in $^4\text{He}/^{232}\text{Th}$ ratios with dust grain size.

Our ability to interpret $^4\text{He}/^{232}\text{Th}$ ratios in these studies is limited by lack of knowledge of $^4\text{He}/^{232}\text{Th}$ ratios in dust source areas and changes in $^4\text{He}/^{232}\text{Th}$ ratios with grain size. Though it is likely that $^4\text{He}/^{232}\text{Th}$ ratios will increase with age in He-retentive source rocks, other potential controls on $^4\text{He}/^{232}\text{Th}$ ratios in source areas – especially weathering intensity and lithology – may complicate a simple relationship with the geological age of source rocks. Additionally, changes in ^4He and ^{232}Th concentrations between dust sources and depositional sites are poorly constrained, raising the question of whether $^4\text{He}/^{232}\text{Th}$ ratios measured in depositional sites reflect dust provenance or are instead affected by size- and density-dependent fractionation during entrainment, transport and deposition. Our study of ^4He and ^{232}Th in dust sources and in downwind ocean sediments provides a starting point for addressing these open questions.

2. STUDY SITES

Samples were collected from dust source areas in East Asia (Sun et al., 2013), Australia (Revel-Rolland et al., 2006; Fitzsimmons et al., 2007; Nanson et al., 2008;

Vallelonga et al., 2010) and South America (Bockheim and Douglass, 2006; Gaiero et al., 2007). Samples in South America are located on the eastern side of the Andean divide and represent two regions that are treated separately in this study: (1) Patagonia (south of 38°S) and (2) the Puna ($\sim 23\text{--}27^\circ\text{S}$) and Central West Argentina ($\sim 28\text{--}32^\circ\text{S}$) region, hereafter Puna-CWA.

Samples were taken from locations thought to best represent the composition of dust exported from each region, typically sediments from dry lake beds, alluvial fan deposits, and loess deposits (Fig. 1; Table EA1). Most samples have been used to represent source areas in previous studies of dust provenance; references for each sample, where available, are listed in Table EA1. All samples were wet sieved to isolate the $<63\ \mu\text{m}$ size fraction, as $>63\ \mu\text{m}$ grains tend to be transported by winds primarily by saltation rather than in suspension and thus have minimal transport distances (Tsoar and Pye, 1987). The $<5\ \mu\text{m}$ fraction, taken to represent dust transported long ($>1000\ \text{km}$) distances, was then separated by settling at LDEO. 63 and $5\ \mu\text{m}$ were chosen to facilitate comparison with other datasets, as these size separations are commonly used in investigations of dust provenance (e.g., Gaiero et al., 2004; Revel-Rolland et al., 2006). For most samples from East Asia, bulk samples were separated into several size fractions by settling in ultrapure water at the State Key Laboratory of Loess and Quaternary Geology in Xi'an. For these samples, the finest grain size fraction is $<4\ \mu\text{m}$.

Samples from 15 ocean sediment cores in which lithogenic fluxes are thought to dominantly derive from eolian dust were analyzed for comparison with dust source area data (Fig. 1; Table EA2). For most cores, three or more samples were analyzed to test for reproducibility of $^4\text{He}/^{232}\text{Th}$ ratios. We attempted to include only samples from the Holocene and late Pleistocene. In regions in which dated cores were not available, we chose piston cores with Pleistocene basal ages and sampled within the top one meter.

For East Asian dust, we chose one loess-paleosol sequence at Zhaojiachuan (ZJC) and two cores (ODP1208, VM32-126) from a region of the North Pacific in which Asian dust has been identified as the dominant source of lithogenic inputs (Nakai et al., 1993; Weber et al., 1996; Jones et al., 2000). We also include results from nine North Pacific coretops studied by Serno et al. (2014) in which rare earth element patterns and grain size data suggest that lithogenic material is $>85\%$ eolian dust.

For Australia, two Tasman Sea cores were chosen (RC9-128, RC9-131). Australian dust is thought to be the dominant source of lithogenic sediments in this region (Hesse, 1994; Kawahata, 2002), though hemipelagic material from New Zealand is an additional potential contributor.

For transport of dust from South America within westerly winds, we chose three south Atlantic cores (VM22-108, RC15-93, RC15-94) in a region where model results indicate that South America is the primary source of dust (Li et al., 2008). Kumar (1994) previously concluded that non-eolian lithogenic inputs were negligible in these cores. Two southeast Pacific cores (ODP1237, VM19-40) were selected to represent South American dust carried by

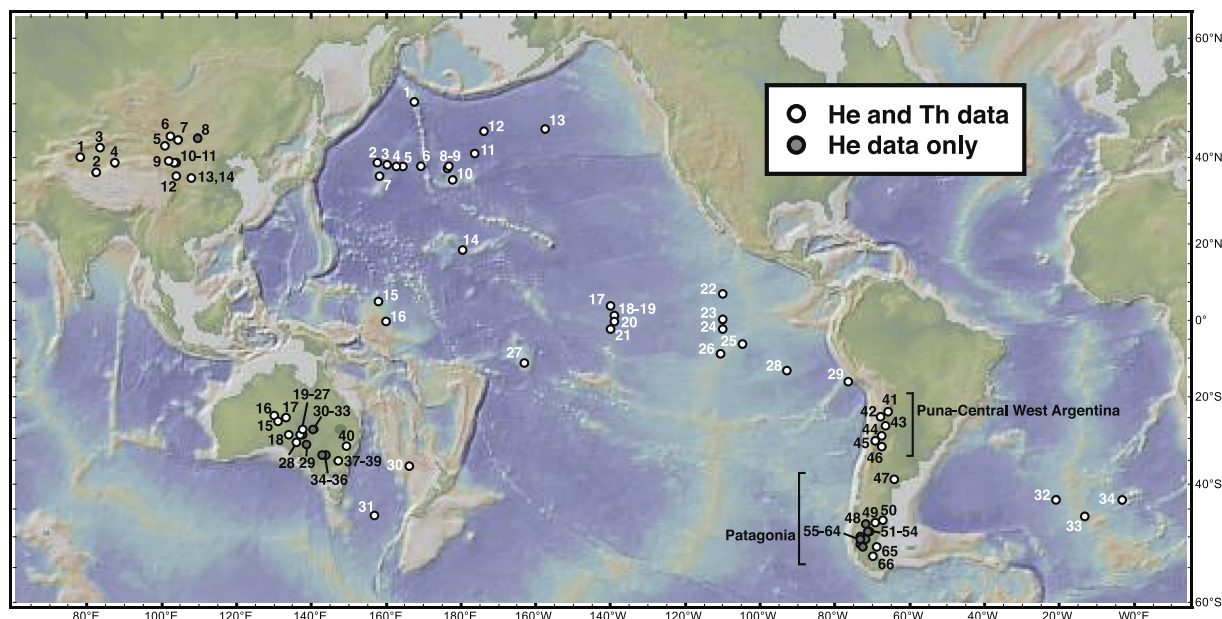


Fig. 1. Map of sample sites. Black numbers (terrestrial sites) refer to locations in [Table EA1](#), and white numbers (marine sites) refer to locations in [Table EA2](#). White dots indicate sites where both He and Th data are available, and grey dots indicate sites where only He data is available. Background map was produced using GeoMapApp (geomapapp.org).

easterly trade winds. These cores lie within a region of high sedimentary quartz abundance tracing a plume of dust reaching northwest from the Altiplano/Atacama region toward the eastern equatorial Pacific ([Molina-Cruz and Price, 1977](#); [Leinen et al., 1986](#)). The grain size distributions and clay mineralogy of surface sediments indicate that eolian dust is the primary contributor of lithogenic sediments at ODP1237, but that sediments near VM19-40 may contain a substantial authigenic component in addition to eolian dust ([Saukel et al., 2011](#)).

We also selected cores in the tropical and equatorial Pacific (ODP853, ODP848, VM21-39, RC10-114, VM24-99) to test for changes in $^4\text{He}/^{232}\text{Th}$ during transport, and we sampled one core in a region of the North Pacific where lithogenic material may include ice-rafted detritus (ODP882). Additionally, we compiled published Th and He isotope data from studies in the Pacific and South Atlantic ([Kumar, 1994](#); [Marcantonio et al., 1996, 2001b](#); [Anderson, 2003](#); [Anderson et al., 2006](#); [McGee et al., 2007](#); [Winckler et al., 2008](#); [Serno et al., 2014](#)).

3. METHODS

3.1. He isotope data

Samples containing high calcium carbonate contents were leached in 0.5 N acetic acid to concentrate detrital material, as carbonate contains negligible He. Dried, homogenized 10–200 mg samples of all sediments were wrapped in Al foil and degassed under vacuum in a Mo crucible at 1200 °C for 15 min. Sample gasses were then purified using a liquid nitrogen-cooled charcoal trap and a Ti getter and captured on a cold head at 14–16 K. He was

released into the MAP 215–50 noble gas mass spectrometer at LDEO for analysis by heating the cold head to 45 K ([Winckler et al., 2005](#)).

^4He abundances and $^3\text{He}/^4\text{He}$ ratios were calibrated using known aliquots of either air standards ($^3\text{He}/^4\text{He} = R_a$) or a ^3He -enriched gas standard (Murdering Mudpot) with $^3\text{He}/^4\text{He} = 16.45 R_a$, where R_a indicates the $^3\text{He}/^4\text{He}$ ratio of the atmosphere (1.384×10^{-6}). Hot blanks were measured for each crucible (i.e., each 3–4 samples) and were $<10^{-9}$ cc STP for ^4He and $<10^{-15}$ cc for ^3He . Blank corrections were $<2\%$ in most samples for both isotopes. ^3He blank corrections for two Australian samples with $^3\text{He}/^4\text{He}$ lower than 10^{-9} were $\sim 50\%$, and as a result we report only upper limits for $^3\text{He}/^4\text{He}$ ratios in these samples. ^4He blank corrections were as high as 8% in equatorial Pacific samples. Uncertainty estimates reflect counting statistics, standard variability and blank corrections, which are assigned a 33% 1-sigma uncertainty.

Ten replicates were measured for dust source area samples, with a ^4He reproducibility of 11%, and nine replicates were measured for sediment core samples, with an average ^4He reproducibility of 21% reflecting their low ^4He concentrations. $^3\text{He}/^4\text{He}$ reproducibility averaged 30% in the dust source area samples and 24% in sediment core replicates. Differences between replicates are thus substantial but are still small relative to the differences between samples. Data from all replicates are included in [Tables EA1 and EA2](#).

In ocean sediments, ^4He inventories are a combination of terrestrial He and He contained in interplanetary dust particles (IDPs). Terrigenous ^4He concentrations ($^4\text{He}_{\text{TERR}}$) were determined using the formula

$$^4\text{He}_{\text{TERR}} = ^4\text{He}_{\text{samp}} \cdot \left(\frac{^3\text{He}/^4\text{He}_{\text{samp}} - ^3\text{He}/^4\text{He}_{\text{IDP}}}{^3\text{He}/^4\text{He}_{\text{TERR}} - ^3\text{He}/^4\text{He}_{\text{IDP}}} \right) \quad (2)$$

where ${}^4\text{He}_{\text{samp}}$ and ${}^3\text{He}/{}^4\text{He}_{\text{samp}}$ are the ${}^4\text{He}$ concentration and ${}^3\text{He}/{}^4\text{He}$ ratio measured in the sample, ${}^3\text{He}/{}^4\text{He}_{\text{IDP}}$ is the isotope ratio in IDPs (see below), and ${}^3\text{He}/{}^4\text{He}_{\text{TERR}}$ is the isotope ratio of terrigenous material ($2\text{--}4 \times 10^{-8}$) (Mamyrin and Tolstikhin, 1984; Farley, 2001).

Following Patterson et al. (1999), we use 4.0×10^{-4} as the ${}^3\text{He}/{}^4\text{He}$ ratio in IDPs. This value is close to the ${}^3\text{He}/{}^4\text{He}$ ratio of solar wind ($\sim 4.5 \times 10^{-4}$; Benkert et al., 1993; Wiens et al., 2004), the primary source of He in IDPs (see review by McGee and Mukhopadhyay, 2013). Some previous studies have used a lower value of 2.4×10^{-4} for ${}^3\text{He}/{}^4\text{He}_{\text{IDP}}$ (e.g., Marcantonio et al., 2009; McGee et al., 2010b) based primarily on measurements of stratospheric IDPs by Nier and Schlutter (1992) and supported by measurements in marine sediments by Marcantonio et al. (2009). In a recent compilation of data from IDPs collected in the stratosphere and from Antarctic ice, most IDPs range from 2×10^{-4} to 4×10^{-4} (McGee and Mukhopadhyay, 2013), suggesting that many IDPs preferentially lose ${}^3\text{He}$ during atmospheric entry and that a value lower than 4×10^{-4} may be a better estimate of ${}^3\text{He}/{}^4\text{He}_{\text{IDP}}$ in sediments. Five sediment samples in this study have ${}^3\text{He}/{}^4\text{He}$ ratios greater than 2.4×10^{-4} (up to 3.0×10^{-4}), supporting use of a higher value for ${}^3\text{He}/{}^4\text{He}_{\text{IDP}}$, but we note that the choice of the best ${}^3\text{He}/{}^4\text{He}_{\text{IDP}}$ in marine sediments is as yet unresolved.

In order to demonstrate the sensitivity of our findings to the choice of ${}^3\text{He}/{}^4\text{He}_{\text{IDP}}$, we calculate ${}^4\text{He}_{\text{TERR}}$ and ${}^4\text{He}/{}^{232}\text{Th}$ ratios in marine sediments using values of 2.4×10^{-4} and 4.0×10^{-4} and report the results in Table EA2. In extratropical sediment cores used in this study, ${}^4\text{He}$ is >90% terrigenous in all samples but one (VM22-108, 13 cm); in these samples, ${}^4\text{He}_{\text{TERR}}$ values are insensitive to the chosen ${}^3\text{He}/{}^4\text{He}$ values of the IDP and terrigenous endmembers. In many samples from the tropical cores, ${}^4\text{He}_{\text{TERR}}$ values are <20% of total ${}^4\text{He}$ and are sensitive to ${}^3\text{He}/{}^4\text{He}_{\text{IDP}}$. Using the lower ${}^3\text{He}/{}^4\text{He}_{\text{IDP}}$ ratio lowers average ${}^4\text{He}_{\text{TERR}}$ concentrations (and thus ${}^4\text{He}_{\text{TERR}}/{}^{232}\text{Th}$ ratios) in these cores by 15–40% in most tropical cores and by 70–90% in two extreme cases in the tropical South Pacific (RC10-114 and RC11-230). The main impact of this change to the findings of this study is to magnify the reduction in ${}^4\text{He}/{}^{232}\text{Th}$ ratios from the extratropics to the tropical Pacific (Section 5.3.3.)

3.2. Thorium data

${}^{232}\text{Th}$ concentrations were measured by isotope dilution at LDEO (Anderson and Fler, 1982; Fleisher and Anderson, 2003). Aliquots of 5–10 mg were taken from larger samples of dried, homogenized sediment were spiked with a ${}^{229}\text{Th}$ – ${}^{236}\text{U}$ solution. Small sample sizes for dust source area samples were required due to limited sample availability, particularly for the fine fraction. A combination of concentrated HClO_4 , HF and HNO_3 were added to dissolve the sample, and the solution was dried down to a viscous bead on a hot plate. A fraction of the samples (18 out of 108) were then taken up in 0.25 N HNO_3 + 0.02 N HF and analyzed after this step. For the majority of the samples, U and Th were removed from solution by Fe

oxy-hydroxide co-precipitation. The samples were then centrifuged and the supernatant decanted to remove other solutes. For most samples, the precipitates were then redissolved in 0.25 N HNO_3 + 0.02 N HF and analyzed. A subset of samples was further purified by anion exchange chromatography prior to being taken up in 0.25 N HNO_3 + 0.02 N HF. No systematic differences were found between the three methods, and replicates processed using the different methods showed similar reproducibility to replicates processed using the same method.

Th isotope abundances were measured using an Axiom single collector ICP-MS at LDEO. ${}^{232}\text{Th}$ concentrations were calculated by using measured ${}^{229}\text{Th}$ counts after corrections for gain, mass bias, blanks and, for ${}^{229}\text{Th}$, tailing from ${}^{230}\text{Th}$ and ${}^{232}\text{Th}$. The average reproducibility of seven replicates was 7%, slightly higher than typical sediment samples (e.g., McGee et al., 2013) likely due to the small aliquots analyzed. This variability between replicates is still small relative to the differences between samples. Data from all replicates are included in Tables EA1 and EA2. The mean of six analyses of the USGS Cody Shale standard (SCo-1) was $8.94 \pm 0.5 \mu\text{g/g}$ (one standard error of the mean), similar to the certified value of $9.7 \pm 0.5 \mu\text{g/g}$. Separate aliquots of six samples included in this study were analyzed by Ferrat et al. (2011) using a different sample dissolution procedure and analysis by standard-sample bracketing on a quadrupole ICP-MS. The mean deviation between Th concentrations measured in the two studies is 13%, with no systematic differences between the two studies.

4. RESULTS

4.1. Helium concentrations and ${}^3\text{He}/{}^4\text{He}$ in terrestrial and marine samples

${}^4\text{He}$ concentrations are relatively consistent in the <63 μm fraction of East Asian loess and desert samples, ranging from 5.7 to 15.6 $\mu\text{cc STP/g}$ (Fig. 2; Table EA1). This value is in good agreement with previous measurements by Farley (2001) and Marcantonio et al. (1998) averaging 6.5 $\mu\text{cc STP/g}$. Concentrations are much higher in <63 μm Australian samples, ranging from 46 to 316 $\mu\text{cc STP/g}$. In South America, ${}^4\text{He}$ concentrations in <63 μm samples displayed a similar mean to East Asian samples but larger variability, with values ranging from 3.0 to 18 $\mu\text{cc STP/g}$ in Patagonia and 0.6–22 $\mu\text{cc STP/g}$ in Puna-CWA.

${}^3\text{He}/{}^4\text{He}$ ratios in dust source area samples generally decrease with increasing ${}^4\text{He}$ concentrations (Figs. 2 and 3). ${}^3\text{He}/{}^4\text{He}$ ratios in East Asian <63 μm samples range from 2.5 to 5.8×10^{-8} , again showing good agreement with the results of Farley (2001) and Marcantonio et al. (1998). Australian <63 μm samples are characterized by very low ${}^3\text{He}/{}^4\text{He}$, with all samples but one having ${}^3\text{He}/{}^4\text{He}$ ratios $<1.2 \times 10^{-8}$, and 2 samples with ${}^3\text{He}/{}^4\text{He} \leq 1 \times 10^{-9}$. In these two samples our values only provide an upper bound to ${}^3\text{He}/{}^4\text{He}$ due to large (up to 50%) ${}^3\text{He}$ blank corrections. South American <63 μm samples again showed high variability, ranging from 2.5×10^{-8} to $>1 \times 10^{-6}$.

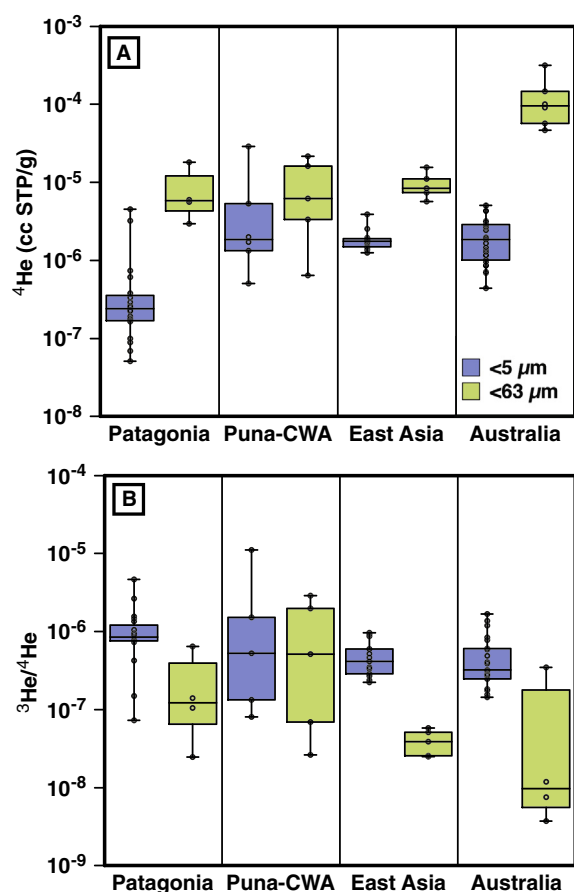


Fig. 2. Box-and-whisker diagrams of (A) ^4He concentrations and (B) $^3\text{He}/^4\text{He}$ ratios of 0–5 μm and 0–63 μm grain size fractions of dust source area samples. Boxes show the two inner quartiles of the data, and whiskers extend to extreme data points. Individual data points are shown as small open circles. Some fine East Asian samples are $<4 \mu\text{m}$ rather than $<5 \mu\text{m}$ (see Table EA1).

Data from finer grain size fractions of source area samples suggest a strong dependence of both ^4He concentrations and $^3\text{He}/^4\text{He}$ on grain size (Figs. 2 and 3). In East Asian samples, ^4He concentrations fall by a factor of ~ 4 with decreasing grain size, from 6.6 to 8.9 $\mu\text{cc STP/g}$ in the two 32–63 μm size fraction samples to an average of 1.8 ± 0.2 (1 standard deviation of the mean) $\mu\text{cc STP/g}$ in the fine (<4 or $<5 \mu\text{m}$) samples. $^3\text{He}/^4\text{He}$ ratios are $3.7\text{--}6.0 \times 10^{-8}$ in the 32–63 μm fractions and average $4.6 \pm 0.8 \times 10^{-7}$ in the fine fraction. ^3He concentrations in East Asian samples are roughly constant in grain size fractions $>8 \mu\text{m}$ and then increase by approximately a factor of 3 in the 4–8 μm and $<4\text{--}5 \mu\text{m}$ size fractions (Fig. 4).

Fine ($<5 \mu\text{m}$) samples from other source areas show similar patterns to the East Asian samples. In Australia, fine samples have an average ^4He concentration of $2.1 \pm 0.3 \mu\text{cc STP/g}$ and an average $^3\text{He}/^4\text{He}$ of $4.5 \pm 0.8 \times 10^{-7}$. In South American samples ^4He concentrations are again substantially lower in $<5 \mu\text{m}$ fractions,

averaging $1.0 \pm 0.3 \mu\text{cc STP/g}$ after exclusion of the fine fraction of sample SA3. The ^4He data from the fine fraction also show geographic differences in South America, with samples from Patagonia averaging $0.8 \pm 0.3 \mu\text{cc STP/g}$, and the samples from Puna-CWA averaging $2.2 \pm 0.8 \mu\text{cc STP/g}$ (again excluding SA3).

$^3\text{He}/^4\text{He}$ ratios in South American samples range to quite high values in both size fractions, up to 2.9×10^{-6} in the $<63 \mu\text{m}$ fraction and 1.1×10^{-5} in the $<5 \mu\text{m}$ fraction. Average $^3\text{He}/^4\text{He}$ ratios in the $<63 \mu\text{m}$ and $<5 \mu\text{m}$ fractions are $7.4 \pm 3.4 \times 10^{-7}$ and $1.35 \pm 0.45 \times 10^{-6}$, respectively. These values are similar to $^3\text{He}/^4\text{He}$ ratios reported from Amazon fan sediments (Marcantonio et al., 1998).

In the marine sediments analyzed for this study, ^4He concentrations range from 0.004 to 1.7 $\mu\text{cc STP/g}$ (Table EA2). These values are lower than in terrestrial sediments due to dilution by calcium carbonate and biogenic opal. $^3\text{He}/^4\text{He}$ ratios range from 2.7×10^{-7} to 3.0×10^{-4} , reflecting mixing between terrigenous He ($^3\text{He}/^4\text{He}$ ratios generally in the range of $10^{-8}\text{--}10^{-6}$) and extraterrestrial He with high $^3\text{He}/^4\text{He}$ ($2.4\text{--}4.0 \times 10^{-4}$) (McGee and Mukhopadhyay, 2013).

4.2. Thorium concentrations in terrestrial and marine sediments

^{232}Th concentrations in the $<63 \mu\text{m}$ source area samples from East Asia and Australia generally fall within 2 ppm of the average for upper continental crust (10.7 $\mu\text{g/g}$; Taylor and McLennan, 1985) and produce averages of 10.8 and 11.3 $\mu\text{g/g}$, respectively (Fig. 5; Table EA1). ^{232}Th concentrations in $<63 \mu\text{m}$ samples from Puna-CWA produce a similar average (10.8 $\mu\text{g/g}$), while those from Patagonia tend to be lower, averaging 8.8 $\mu\text{g/g}$. These findings are quite similar to a previous estimate of ^{232}Th concentrations in dust sources based on published analyses of $<63 \mu\text{m}$ samples (McGee et al., 2007).

^{232}Th concentrations consistently rise with decreasing grain size. Average ^{232}Th concentrations in fine fraction samples (<4 or $<5 \mu\text{m}$) are $13.6 \pm 2.8 \mu\text{g/g}$ (South America), $13.7 \pm 0.8 \mu\text{g/g}$ (East Asia) and $16.8 \pm 2.8 \mu\text{g/g}$ (Australia) (Fig. 5). Excluding a fine fraction sample with an extremely high Th concentration (AU5) produces an average of $14.3 \pm 1.3 \mu\text{g/g}$ in Australia. As with ^4He , there may be geographic differences in fine fraction ^{232}Th concentrations in South America, with lower ^{232}Th concentrations in Patagonia ($9.4 \pm 1.7 \mu\text{g/g}$) and higher concentrations in Puna-CWA ($17.1 \pm 3.7 \mu\text{g/g}$). Size fraction samples from East Asia spanning the $<63 \mu\text{m}$ range show the impact of grain size on ^{232}Th concentrations in more detail, as ^{232}Th concentrations rise by a factor of 2–3 between the 32 and 63 μm and $<4 \mu\text{m}$ size fractions (Fig. 3).

^{232}Th concentrations in marine sediments are lower than in terrigenous sediments due to dilution by biogenic sediments, ranging from a minimum of 0.08 $\mu\text{g/g}$ in the tropical Pacific to a maximum of 12.3 $\mu\text{g/g}$ in the North Pacific (Table EA2).

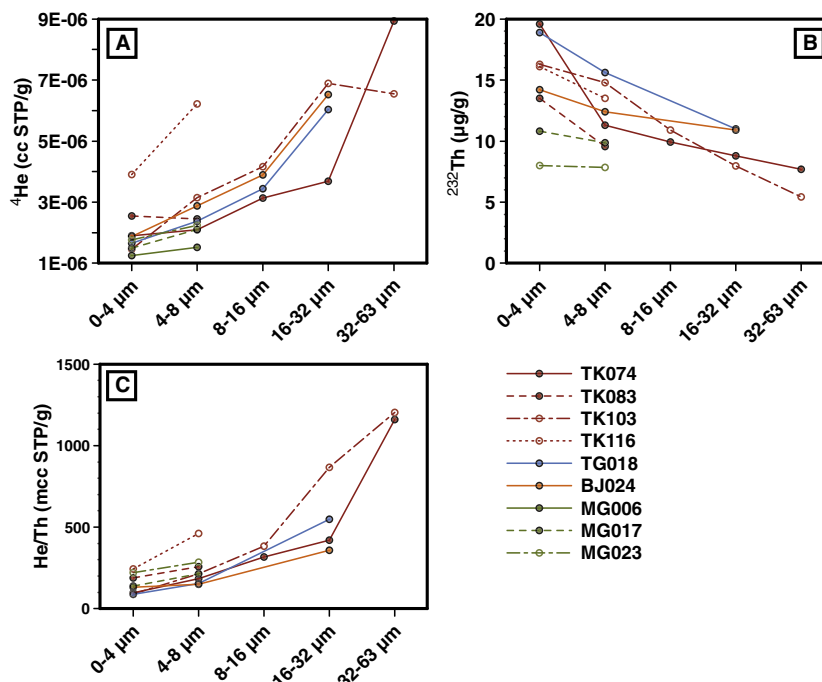


Fig. 3. Impact of grain size on (A) ^4He concentrations, (B) ^{232}Th concentrations, and (C) $^4\text{He}/^{232}\text{Th}$ ratios in samples from East Asian dust source areas. Locations of samples are given in Table EA1.

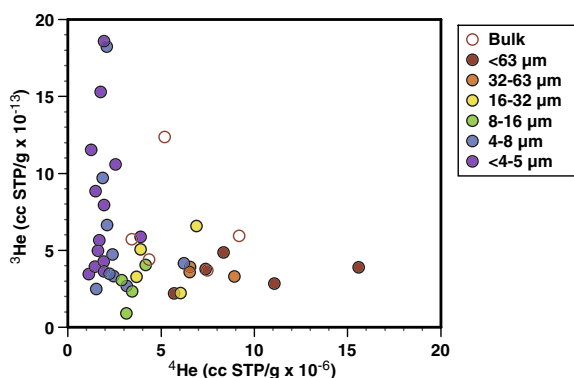


Fig. 4. Comparison of changes in ^3He and ^4He concentrations with grain size in Chinese source area samples. ^4He concentrations drop with decreasing grain size, as shown in Fig. 3. ^3He concentrations stay roughly constant until grain sizes drop to $\sim 8\ \mu\text{m}$, after which ^3He concentrations increase.

5. DISCUSSION

5.1. Helium concentrations and isotopic composition in dust source area samples

We observe a pronounced decrease in ^4He concentrations and increase in $^3\text{He}/^4\text{He}$ ratios with decreasing grain size in dust source area samples from East Asia, Australia, and South America (Figs. 2 and 3). In the $<63\ \mu\text{m}$ fraction, we observe substantial differences in He concentrations and isotopic compositions between source areas. Australian $<63\ \mu\text{m}$ samples have ^4He concentrations that are

substantially higher, and $^3\text{He}/^4\text{He}$ ratios that are substantially lower, than samples from other source areas. In the fine ($<5\ \mu\text{m}$) fraction, however, ^4He concentrations are very similar, with mean values from East Asia, Australia and Puna-CWA all within uncertainty of $2\ \mu\text{cc STP/g}$, and Patagonia lower at approximately $0.8\ \mu\text{cc STP/g}$. In the following sections we explore potential explanations for, and implications of, these results.

5.1.1. Helium in coarse ($<63\ \mu\text{m}$) fractions of the sediment

^4He in the upper continental crust is dominantly produced as alpha particles from U and Th decay. In granite and other source rocks, U and Th are concentrated in accessory mineral phases such as zircon, amphibole, uraninite and monazite (e.g., Martel et al., 1990), all of which have sufficient He retentivity to have much higher ^4He concentrations than bulk rock (Mamyrin and Tolstikhin, 1984; Lippolt and Weigel, 1988; Martel et al., 1990). In the $<63\ \mu\text{m}$ fractions, which are likely to have undergone minimal chemical alteration and to be composed of primary rock-forming minerals (e.g., Jeong et al., 2008; Meyer et al., 2013), it is thus likely that ^4He will be primarily contained in these accessory mineral phases.

Dominant minerals such as quartz, feldspar and mica often have ^4He concentrations on the order of $1\text{--}10\ \mu\text{cc STP/g}$ when measured as coarse-grained ($\sim 1\ \text{mm}$) mineral separates from source rocks (Mamyrin and Tolstikhin, 1984; Martel et al., 1990; Tolstikhin et al., 1996). These concentrations are similar to those measured in dust source samples in this study (excluding $<63\ \mu\text{m}$ samples from Australia), suggesting that He in some dust source areas may be contained in dominant minerals rather

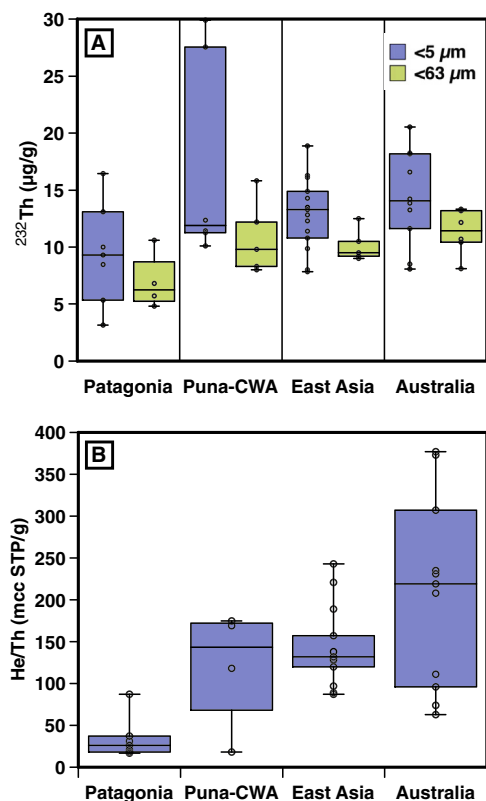


Fig. 5. Th concentrations and He/Th ratios in samples from different dust source areas. (A) Box-and-whisker diagram of Th concentration data for two size fractions of terrestrial dust source area samples from Patagonia, Puna-Central West Argentina, East Asia and Australia. Data from $<5\ \mu\text{m}$ fraction are shown in blue, and data from the $<63\ \mu\text{m}$ fraction are shown in green. Boxes indicate the middle two quartiles of the data distribution, and whiskers extend to the extreme data points. Some East Asian fine fraction data are from the $<4\ \mu\text{m}$ fraction (see Table EA1). (B) He/Th ratios in the fine fraction of sediments from the four dust source areas. (For interpretation of the references to colour in this figure legend, the reader is referred to the web version of this article.)

than accessory phases. This possibility is made less likely, however, by the high measured diffusivities of quartz, potassium feldspar (sanidine) and mica (muscovite), which indicate that He is largely lost from silt- and clay-sized grains of these minerals over geologic (10^5 – 10^6 yr) time scales (Table 1). Our calculations use the equation of Mussett (1969) for calculating the fraction of initial He lost (F_1) from minerals:

$$F_1 = 1 - \frac{6}{\pi^2} \exp\left(\frac{-\pi^2 Dt}{a^2}\right) \quad (3)$$

where t is time, a is the grain radius, and D is the diffusivity of the mineral phases at a given temperature. D is calculated using

$$D(T) = D_0 \exp\left(\frac{-E_a}{RT}\right) \quad (4)$$

where D_0 is the diffusivity at infinite temperature, E_a is the activation energy, R is the universal gas constant and T is temperature in Kelvin. Table 1 includes calculations of

the time required to lose 90% of initial He for $2\ \mu\text{m}$ and $30\ \mu\text{m}$ grains of various mineral phases at surface ($20\ ^\circ\text{C}$) and seafloor ($2\ ^\circ\text{C}$) temperatures. Loss times for $2\ \mu\text{m}$ grains of zircon, amphibole (hornblende) and iron oxyhydroxides (goethite) are all $>10^7$ years, while those for quartz, feldspar and mica are all $<10^5$ years. Raising the temperature to $40\ ^\circ\text{C}$ to reflect high daytime temperatures in deserts results in a factor of ~ 10 decrease in loss times (not shown); for zircon, amphibole and iron oxyhydroxides even this $>10^6$ year timescale – which assumes constant $40\ ^\circ\text{C}$ heating – is long relative to the typical residence time of grains at the Earth's surface. Trace phases such as apatites, titanite and rutile also have high He retentivity at surface temperatures (Reiners and Farley, 1999; Farley, 2002; Cherniak and Watson, 2011).

We now turn our attention to the substantial (factor of ~ 20) enrichment in ^4He in Australian $<63\ \mu\text{m}$ samples relative to samples from East Asia (Fig. 2). The preceding discussion would suggest that ^4He concentrations in $<63\ \mu\text{m}$ source area samples should reflect the prevalence and age of U and Th-rich accessory mineral phases such as zircon, as suggested by Patterson et al. (1999). U–Pb dating of zircons in sand dunes in 3 sites spread across south-central Australia indicates that the largest concentration of dates lies between 1.0 and 1.7 Ga (Pell et al., 1997), while zircons in Chinese loess date to 200–500 Ma (Pullen et al., 2011). This factor of ~ 2 – 8 difference in age could be an important contributor to higher ^4He concentrations in Australian $<63\ \mu\text{m}$ source area sediments. Zr concentrations are approximately equal in Chinese loess and in Australian surface samples (~ 170 ppm; Jahn et al., 2001; Marx et al., 2005a,b); assuming that Zr concentrations are a rough proxy for zircon abundance, these data would suggest that the abundance of zircons does not explain the difference in ^4He concentrations between the two regions.

In addition to a potential age difference, differences in ^4He concentrations between Australian and East Asian $<63\ \mu\text{m}$ samples may reflect differences in the prevalence of other ^4He -retentive phases (e.g., amphiboles, iron oxides and oxyhydroxides), in the grain size distribution within the $<63\ \mu\text{m}$ fraction, or in chemical weathering.

$^3\text{He}/^4\text{He}$ ratios in $<63\ \mu\text{m}$ samples from East Asia range from 2.5 to 5.8×10^{-8} , consistent with average production ratios for the upper continental crust calculated based on production of ^4He by U and Th decay and production of ^3He primarily by the $^6\text{Li}(n,\alpha)^3\text{H}$ reaction (after which ^3H decays to ^3He) (Morrison and Pine, 1955; Andrews, 1985). The equivalence of calculated and measured $^3\text{He}/^4\text{He}$ ratios in East Asian samples suggests that nucleogenic ^3He and radiogenic ^4He have been retained approximately equally in these grains.

In Australia, $^3\text{He}/^4\text{He}$ ratios in 5 of 6 $<63\ \mu\text{m}$ samples are roughly an order of magnitude lower than in East Asia, with the only exception being one high- $^3\text{He}/^4\text{He}$ sample from the Lake Eyre basin (AU1) (Fig. 2). It does not appear likely that ^3He production rates are significantly lower in the Australian samples than in the Chinese samples. ^3He production depends to first order on the thermal neutron flux, a function both of mineralogy and of U and Th concentrations, and on Li concentrations. Analyses of source

Table 1

Calculations of the length of time before various minerals lose 90% of He, based on published diffusion coefficients and calculated using the He retention equation for >85% loss of Crank (1957) as reported in Table 1 of Mussett (1969). 2 μm grains of quartz, mica (muscovite) and feldspar (sanidine) retain He for <1 Myr at temperatures typical of the bottom of the ocean, while goethite (iron oxyhydroxide) amphibole (hornblende) and zircon retain He for geologically long periods. Note that the values for goethite do not vary with grain size because experimental results suggest that diffusion domains are smaller than grain sizes; the present results assume domains of 0.5 μm . (Shuster et al. (2005)). The diffusion coefficients used for quartz are 2–5 orders of magnitude lower than estimates in other studies (Brook and Kurz, 1993; Shuster and Farley, 2005) and were chosen to provide an upper limit on the duration of He retention in quartz.

Mineral	Temperature ($^{\circ}\text{C}$)	Time of 90% He loss (y)		Reference for diffusion coefficient
		Grain size	Grain size	
		30 μm	2 μm	
Zircon	20	3.8×10^{16}	1.7×10^{14}	Reiners et al. (2004)
	2	3.6×10^{18}	1.6×10^{16}	
Hornblende	20	2.6×10^9	1.2×10^7	Lippolt and Weigel (1988)
	2	6.6×10^{10}	2.9×10^8	
Goethite	20	2.5×10^{11}	2.5×10^{11}	Shuster et al. (2005)
	2	2.0×10^{13}	2.0×10^{13}	
Sanidine	20	1.6×10^6	7.3×10^3	Lippolt and Weigel (1988)
	2	2.1×10^7	9.1×10^4	
Muscovite	20	3.7×10^5	1.6×10^3	Lippolt and Weigel (1988)
	2	3.8×10^6	1.7×10^4	
Quartz	20	5.4×10^4	2.4×10^2	Trull et al. (1991)
	2	9.1×10^5	5.8×10^3	

area sediments in both regions do not suggest significant differences in U, Th or Li concentrations (Jahn et al., 2001; Marx et al., 2005a,b), and the measured Th concentrations of these samples are not significantly different (Fig. 5). It should be noted that ^3He production also depends on the concentration of elements that efficiently absorb neutrons – e.g., B, Cd, Gd – which may account for some of the difference in $^3\text{He}/^4\text{He}$ ratios. However, it is also possible that a much higher proportion of radiogenic ^4He is retained relative to nucleogenic ^3He in Australian source rocks. A similar pattern has been observed in granites in England with whole rock $^3\text{He}/^4\text{He}$ ratios of $1.5\text{--}4.8 \times 10^{-9}$, similar to values in our Australian samples and more than an order of magnitude lower than the production rate calculated for these granites assuming homogeneous element distributions (5.4×10^{-8} ; Hilton, 1986). Martel et al. (1990) related these low whole-rock ratios to the fact that the majority of the rock's U and Th are in He-retentive accessory minerals such as uraninite and monazite, while the majority of Li (and thus ^3He production) is in biotite, a mineral with low He retentivity. As a result, nucleogenic ^3He is lost preferentially to radiogenic ^4He . Differences in $^3\text{He}/^4\text{He}$ ratios in source areas may thus reflect differences in mineralogy and weathering, and not simply geological age or $^3\text{He}/^4\text{He}$ production rates.

The variable ^4He concentrations found in South America likely reflect contrasts between late Cenozoic volcanics in Patagonia that are likely to be ^4He -poor (Gaiero et al., 2004) and ^4He -enriched rocks such as Precambrian through Mesozoic igneous and metasedimentary rocks in Puna-CWA or Jurassic rhyolites in parts of Patagonia (Allmendinger et al., 1997; Gaiero et al., 2007). This difference parallels the much more radiogenic Nd isotopic composition of Patagonian surface deposits compared to samples from Central Western Argentina and the Puna-Altiplano Plateau (Gaiero, 2007), indicating that

the younger mean age of bedrock in Patagonia may explain the lower ^4He concentrations there. $^3\text{He}/^4\text{He}$ ratios in South American <63 μm samples are also variable and range up to 10^{-6} , far higher than likely rates of radiogenic and nucleogenic He production in these grains. Marcantonio et al. (1998) attributed high $^3\text{He}/^4\text{He}$ ratios in Amazon fan sediments to mantle-derived He, which has been suggested as a significant contributor to total He even in geologically old samples (Mamyrin and Tolstikhin, 1984). Farley (2001) argued, however, that mantle He should be lost during physical weathering, and instead attributed the $^3\text{He}/^4\text{He}$ component to extraterrestrial He hosted by IDPs deposited on the landscape and accumulated within detrital sediments. We cannot reject Farley's hypothesis, but we note that high ($>10^{-6}$) $^3\text{He}/^4\text{He}$ ratios are found even in glaciogenic South American sediments with little opportunity for IDP accumulation (e.g., SMD2, FG1, MK3; Table EA1).

Cosmogenic ^3He is an additional potential contributor to high $^3\text{He}/^4\text{He}$ ratios in South American sediments. Farley (2001) suggested that cosmogenic ^3He is unlikely to be important in terrestrial sediments, reasoning that olivine and pyroxene, retentive phases that are the dominant hosts of cosmogenic ^3He , are easily weathered and likely to lose He after being separated from source rocks (Farley, 2001). Phases such as amphiboles, iron oxides, iron oxyhydroxides, apatites, and rutiles that are more resistant to weathering may also accumulate cosmogenic ^3He , potentially contributing to high $^3\text{He}/^4\text{He}$ ratios in South America. It is not clear, however, why cosmogenic ^3He would drive high $^3\text{He}/^4\text{He}$ ratios in South American sediments but not lead to high $^3\text{He}/^4\text{He}$ ratios in Australian and East Asian sediments.

5.1.2. Helium in fine (<5 μm) fractions of the sediment

Here we address the questions of (1) why ^4He concentrations drop and $^3\text{He}/^4\text{He}$ ratios rise with decreasing grain

size and (2) what phases are the dominant carriers of ^4He in the fine fraction. Several possible mechanisms related to physical and chemical weathering may contribute to the substantial decrease in ^4He concentrations with decreasing grain size (Fig. 3). First, as grain sizes decrease during physical weathering, losses of ^4He increase due to a combination of diffusion and recoil loss. Diffusive losses increase in proportion to $1/a^2$, where a is the radius of the diffusion domain, which in most cases is the mineral grain (Mussett, 1969). Fractures sustained during physical weathering further increase diffusive losses by effectively increasing grain surface area (Ballentine and Burnard, 2002). Recoil lengths for alpha particles range from 10 to 30 μm , depending on grain density and chemistry; all newly produced alpha particles are thus ejected from grains in fine silt- and clay-sized grains. In these fine-grained sediments, alpha particles are often implanted in neighboring grains, but as this implanted ^4He is connected to pore spaces by a damage track, its diffusivity is much higher than if it were retained in the parent mineral (Ballentine and Burnard, 2002). Consequently, radiogenic ^4He produced in clay-sized grains is quantitatively lost to surrounding porewaters (Farley, 1995; Solomon et al., 1996; Tolstikhin et al., 1996).

In addition to increased diffusive and recoil losses in fine grains, He concentrations may be reduced by mineral diagenesis associated with chemical weathering. As He behaves incompatibly during mineral alteration, its loss during the formation of secondary clay minerals is contingent only on having a pathway to escape (Ballentine and Burnard, 2002). The prevalence of these low- ^4He secondary clay minerals increases with decreasing grain size (e.g., Jeong et al., 2008; Meyer et al., 2013), providing an additional mechanism for reduced ^4He concentrations in fine-grained material.

Though ^4He loss is likely a dominant driver of the decline in ^4He concentrations with decreasing grain size, variations in ^4He concentrations within the fine fraction may still reflect differences in ^4He production related to the composition and age of source rocks. Sr, Nd and Pb isotopic data are available for the $<5\ \mu\text{m}$ fractions of a subset of the Australian measured in this study (Revel-Rolland et al., 2006; Vallelonga et al., 2010) (Table EA1). Sr and Nd isotopic ratios in Australian samples show significant correlations with ^4He ($r = 0.66$, $p < 0.05$ for Sr; $r = 0.53$, $p < 0.1$ for Nd) (Fig. 6), with higher ^4He concentrations associated with higher $^{87}\text{Sr}/^{86}\text{Sr}$ and more negative ϵ_{Nd} values. This correlation may derive from the fact that samples with more radiogenic Sr and more negative ϵ_{Nd} are likely to be geologically older and/or from lithologies more enriched in incompatible trace elements; both of these characteristics would lead to higher ^4He concentrations. No significant correlations were observed between radiogenic isotope data and $^3\text{He}/^4\text{He}$ ratios, $^4\text{He}/^{232}\text{Th}$ ratios or ^{232}Th concentrations in the fine fraction where data exist, nor was the correlation between Pb isotope ratios and ^4He concentrations significant.

As fine fraction ^4He is only a small portion of total source rock ^4He , it is unclear what minerals are the dominant host of ^4He in the fine fraction. Analysis of the $<2\ \mu\text{m}$ fractions of both aerosol and deep-sea sediment

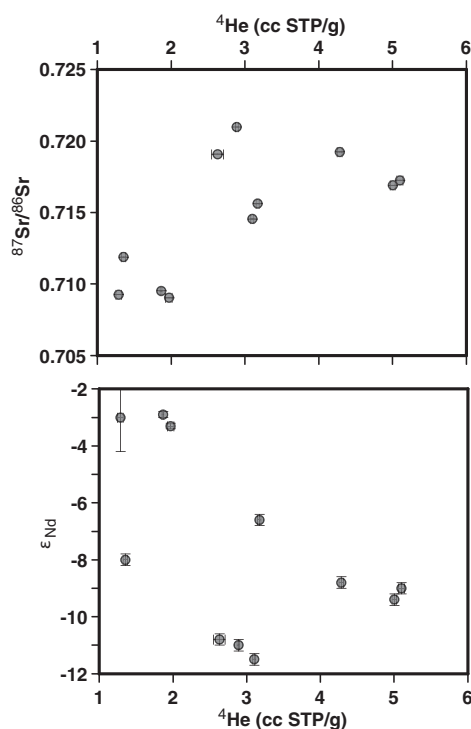


Fig. 6. Correlations between ^4He concentrations and Sr and Nd isotopic data from the fine fractions of Australian source area sediments. Sr (top) and Nd (bottom) data are from Revel-Rolland et al. (2006). All radiogenic isotope data are included in Table EA1. 95% confidence intervals are shown for radiogenic isotope data.

samples from the North Pacific indicates that they are comprised almost entirely of minerals with low ^4He retentivity: quartz, plagioclase, illite, kaolinite and chlorite (Blank et al., 1985). It appears that ^4He in long-traveled dust is contained in a highly retentive phase, as ^4He concentrations in detrital material in a North Pacific core fall by only a factor of 2 over the Cenozoic (Farley, 1995). Patterson et al. (1999) suggested that most ^4He in distal marine sediments is contained in zircons, which are known to have extremely high ^4He abundances and retentivity.

We argue, however, that phases with moderate He contents and greater abundance in fine-grained sediments such as iron oxides, iron oxyhydroxides and amphiboles are more likely carriers for He in the fine fraction of terrestrial sediments and dust. As shown in Table 1, these phases (represented by hornblende and goethite) have sufficiently high He retentivity to be consistent with the observation that ^4He is retained in marine sediments over tens of millions of years (Farley, 1995).

A first piece of evidence against zircon as the primary carrier of He in the fine fraction comes from leaching experiments conducted on red clay sediments from the North Pacific, which found that $\sim 80\%$ of terrestrial ^4He was lost on leaching with 6 M HCl at room temperature (Mukhopadhyay and Farley, 2006). Zircon is a highly resistant mineral not prone to dissolution in HCl (Krogh, 1973), while iron oxides and oxyhydroxides are readily dissolved

by HCl (Schwertmann, 1991). Amphiboles also show measurable weathering by HCl (Frogner and Schweda, 1998).

Second, the substantial increase in $^3\text{He}/^4\text{He}$ with decreasing grain size also argues against zircon and other U-rich trace phases as the primary carriers of He in the fine fraction. These phases are exceptionally rich in radiogenic ^4He and tend to have very low $^3\text{He}/^4\text{He}$ ratios (typically $\ll 1 \times 10^{-8}$ for zircons) (e.g., Amidon and Farley, 2011). Our results suggest that ^3He concentrations initially remain roughly constant as ^4He concentrations decrease with decreasing grain size, then rise in the finest fractions (4–8 μm and $<4\text{--}5 \mu\text{m}$) (Fig. 4). This observation, along with the high $^3\text{He}/^4\text{He}$ ratios measured in the fine fraction, suggests that ^3He -rich minerals are concentrated in the fine fraction. ^3He production tends to be concentrated in micas in igneous and metamorphic rocks due to their high Li concentrations (Section 5.1.1), but micas tend to have low He concentrations due to their high He diffusivities. As a result, studies of mineral separates from intrusive igneous rocks find that the majority of ^3He is in minerals with only moderate Li concentrations but low He diffusivity, often amphibole (Mamyrin and Tolstikhin, 1984). Amphiboles have been observed to contain ^3He in excess of production and $^3\text{He}/^4\text{He}$ ratios of $\sim 10^{-7}$ (Mamyrin and Tolstikhin, 1984) and are thus a plausible source of high ^3He in the fine fraction.

Literature data allow us to assess whether amphiboles and iron oxides/oxyhydroxides can account for most or all of the $\sim 2 \mu\text{cc STP/g}$ ^4He concentrations we find in the fine fractions of dust source area samples. Jeong et al. (2008) found that amphiboles and iron oxides/oxyhydroxides comprise approximately 2% and 1.5%, respectively, of mineral grains in loess deposits at the western margin of the Chinese loess plateau. Lippolt and Weigel (1988) reported that hornblendes dated by K–Ar geochronology to 240 Ma have ^4He concentrations of $30 \mu\text{cc STP/g}$. If these hornblende data are roughly representative of amphiboles in general, and if dust transported over long distances contains $\sim 2\%$ amphiboles, then amphiboles with a mean age of ~ 800 Ma would produce a ^4He concentration in long-traveled bulk dust of $\sim 2 \mu\text{cc STP/g}$, as observed in this study for the fine fraction of dust from a variety of source areas. Similarly, ^4He concentrations in 40 Ma goethites studied by Shuster et al. (2005) are high enough ($> 2 \times 10^{-4}$ cc STP/g) that a 1% abundance of similar iron oxyhydroxides in dust would result in a He concentration of $2 \mu\text{cc STP/g}$. These calculations demonstrate that phases such as amphiboles and iron oxides/oxyhydroxides, which have percent-level abundances in dust deposits (e.g., Jeong et al., 2008), moderate He contents and high He retentivity, may be the dominant carriers of He in fine dust rather than extremely He-rich trace phases such as zircon. Iron oxides/oxyhydroxides are likely to be a more important carrier of helium in the fine fraction than amphiboles due to their more rapid accumulation of radiogenic ^4He .

High $^3\text{He}/^4\text{He}$ in the fine fraction could potentially come from interplanetary dust particles (IDPs) containing extraterrestrial He, as He-retentive IDPs in marine sediments and polar ice are dominantly fine-grained (Mukhopadhyay and Farley, 2006; Brook et al., 2009;

McGee et al., 2010b). However, little is known about the He retentivity of IDPs subjected to terrestrial weathering, and as noted above (Section 5.1.1) even glaciogenic sediments with little opportunity for IDP accumulation show high $^3\text{He}/^4\text{He}$ ratios. Cosmogenic ^3He is also a potential contributor to high $^3\text{He}/^4\text{He}$ in the fine fraction, as discussed for coarse sediments in Section 5.1.1. However, even zircons with exposure ages of $> 10^4$ yr have $^3\text{He}/^4\text{He} < 1 \times 10^{-8}$ (Amidon and Farley, 2011).

Regardless of its cause, the simple observation that $^3\text{He}/^4\text{He}$ ratios are typically in the range of 10^{-7} to 10^{-6} in the fine fraction of dust source area sediments has important implications for studies of extraterrestrial ^3He in marine sediments and ice cores, as these studies use an estimate of the terrigenous $^3\text{He}/^4\text{He}$ ratio to determine extraterrestrial He concentrations. This point is explored in more detail in the following section.

5.1.3. Implications for studies involving ^4He in dust and extraterrestrial ^3He

Our measurements of ^4He concentrations and $^3\text{He}/^4\text{He}$ ratios in different size fractions and dust source areas have implications both for He as a dust tracer and for studies involving extraterrestrial ^3He . For dust reconstructions in distal sites such as open-ocean sediments and ice cores where dust is dominantly fine-grained, our results suggest relatively homogenous ^4He concentrations in the $< 5 \mu\text{m}$ fraction of dust from East Asia, Australia and Puna-CWA, all of which average $\sim 2 \mu\text{cc STP/g}$. The exception is Patagonia, where ^4He concentrations appear to be lower ($\sim 0.8 \mu\text{cc STP/g}$) and more variable. The consistency of these results suggests that dust fluxes may be estimated from ^4He fluxes at sites where dust is dominantly fine-grained. However, in sites with a range of dust grain sizes (i.e., sites $< \sim 500$ km from source areas; Tsoar and Pye, 1987), the strong dependence of ^4He concentrations on grain size complicates the use of ^4He for quantitatively estimating dust accumulation rates in sediments. Interpretation of ^4He -based provenance tracers such as $^4\text{He}/\text{Ca}$, $^3\text{He}/^4\text{He}$ and $^4\text{He}/^{232}\text{Th}$ ratios will be similarly affected by the grain size dependence of ^4He concentrations in source-proximal deposits.

These data also have important implications for studies involving extraterrestrial ^3He . In order to deconvolve extraterrestrial from terrigenous He, studies must assume a $^3\text{He}/^4\text{He}$ ratio of terrigenous matter, typically $1\text{--}4 \times 10^{-8}$ based in part on measurements of bulk Chinese loess (Farley and Patterson, 1995; Marcantonio et al., 1998; Farley, 2001). Our data suggest that in regions where fine-grained dust forms a dominant source of terrigenous sediments, the terrigenous $^3\text{He}/^4\text{He}$ ratio may be an order of magnitude higher, in the range of $4\text{--}5 \times 10^{-7}$ for East Asian and Australian sources and 10^{-6} for South American sources. It is recommended that studies estimating extraterrestrial ^3He concentrations in sediments explore the sensitivity of their results to higher terrigenous $^3\text{He}/^4\text{He}$ ratios. In cases where the results show substantial sensitivity, efforts should be made to constrain the terrigenous $^3\text{He}/^4\text{He}$ ratio, either through physical (e.g., magnetic) concentration of the terrestrial fraction or through measurement of

samples that represent the grain size and provenance of the terrigenous endmember. Further work should also explore whether there are ways of constraining the $^3\text{He}/^4\text{He}$ ratio of the terrigenous endmember based on independent measurements such as grain size and elemental composition (e.g., U, Th, Li).

5.2. Thorium concentrations in dust sources and implications for dust flux reconstructions

We find a consistent increase in ^{232}Th concentrations with decreasing grain size, with mean concentrations of $14 \pm 1 \mu\text{g/g}$ (error-weighted mean) in fine (<4 or $<5 \mu\text{m}$) samples from East Asia, Australia and Puna-CWA (Figs. 3 and 4). This value is approximately 30% higher than the mean concentration in the $<63 \mu\text{m}$ fractions of samples from East Asia and Australia, and 60% higher than in $<63 \mu\text{m}$ samples from South America. The fine fraction of African dust appears to have a similar ^{232}Th concentration, as the average ^{232}Th concentration of the 0–2 μm and 2–5 μm fractions of African dust collected in Barbados is $13.6 \mu\text{g/g}$ (Muhs et al., 2007). African dust also shows a similar increase of ^{232}Th concentrations with decreasing grain size; concentrations in Barbados dust were 30% higher in the 0–2 μm fraction than in the 10–20 μm fraction (Muhs et al., 2007). A similar pattern with grain size is seen in dust source area samples from Africa (Castillo et al., 2008).

Increased ^{232}Th concentrations in fine sediments may result from a reduced proportion of low- ^{232}Th phases such as quartz and feldspar in fine sediments (e.g., Leinen et al., 1994; Jeong et al., 2008; Meyer et al., 2013); as an example, Jeong et al. (2008) found that bulk Chinese loess was 50–60% quartz and feldspar, while the $<2 \mu\text{m}$ fraction was $\sim 80\%$ illite and smectite. Additionally, during chemical weathering the low solubility of Th may cause it to remain adsorbed to clay minerals or Fe–Mn oxides as other ions are leached from the sediments (Marchandise et al., 2014).

Given the similar ^{232}Th concentrations in the fine fraction of dust source area samples from East Asia, Australia, South America (this study) and Africa (Muhs et al., 2007), we recommend that studies using ^{232}Th fluxes to estimate dust fluxes in distal sediments assume a ^{232}Th concentration of $14 \pm 1 \mu\text{g/g}$ in dust. Several previous studies have used an estimate of the average ^{232}Th concentration of the upper continental crust ($10.7 \mu\text{g/g}$; Taylor and McLennan, 1985) to calculate dust fluxes (e.g., Anderson et al., 2006; McGee et al., 2007; Winckler et al., 2008; Martínez-García et al., 2009); these studies may systematically overestimate dust fluxes by $\sim 30\%$ in regions where dust is dominantly $<5 \mu\text{m}$. In studies attempting to quantitatively estimate detrital concentrations and fluxes using ^{232}Th concentrations, it is best to base these estimates on ^{232}Th concentrations in the appropriate grain size and detrital provenance rather than using the average concentration in upper continental crust.

An exception to this recommendation should be made for sites receiving exclusively fine Patagonian dust, which our data suggest has a lower ^{232}Th concentration ($\sim 9 \mu\text{g/g}$), in agreement with previous work (Gaiero et al., 2004,

2007). This lower Th concentration appears to result from contributions of basaltic to basaltic-andesitic composition volcanics from the Southern Volcanic Zone; a ~ 60 – 40 mixture between these low-Th volcanics and high-Th Jurassic rhyolites found in the region explains well the chemical and isotopic signature of Patagonian sediment and dust (Gaiero et al., 2007).

5.3. $^4\text{He}/^{232}\text{Th}$ ratios as a dust provenance tracer

5.3.1. Changes in $^4\text{He}/^{232}\text{Th}$ with grain size and between source areas

As a result of the relative constancy of ^{232}Th concentrations in terrestrial samples, variability in $^4\text{He}/^{232}\text{Th}$ ratios is primarily driven by ^4He concentrations. We express $^4\text{He}/^{232}\text{Th}$ ratios in the unit of mcc STP/g, as this ratio is a simple division of ^4He concentration data in common units of ncc STP/g by ^{232}Th concentrations in units of $\mu\text{g/g}$. This unit also has the advantage that most fine fraction and marine sediment values fall in the range of 10–200, as opposed to 0.01 to 0.20 if the unit were cc STP/g. $^4\text{He}/^{232}\text{Th}$ ratios can be converted to atomic ratios by multiplying values in mcc STP/g by 1.0352×10^{-5} .

In the $<63 \mu\text{m}$ fraction, $^4\text{He}/^{232}\text{Th}$ ratios in Australian samples are consistently higher than in samples from East Asia and South America. Australian $^4\text{He}/^{232}\text{Th}$ ranges from 4320 to 25,800 mcc STP/g; Chinese $^4\text{He}/^{232}\text{Th}$ in $<63 \mu\text{m}$ samples ranges from 457 to 1480 mcc STP/g; and South America shows the greatest variability, with ratios ranging from 53 to 2680 mcc STP/g (Table EA1). Fine fraction $^4\text{He}/^{232}\text{Th}$ ratios, which are more likely to reflect values in long-traveled dust, are significantly lower and less variable. $^4\text{He}/^{232}\text{Th}$ ratios in the fine fraction average 209 ± 34 mcc STP/g in Australian samples, 142 ± 14 mcc STP/g in East Asian samples, 132 ± 30 mcc STP/g in Puna-CWA (after exclusion of SA3), and 44 ± 10 mcc STP/g in Patagonia.

Consistent with the difference in $^4\text{He}/^{232}\text{Th}$ between the <5 and $<63 \mu\text{m}$ size fractions from each source area, the two full sets of grain size fractions from East Asia demonstrate a strong dependence of $^4\text{He}/^{232}\text{Th}$ on grain size. Increasing ^{232}Th and decreasing ^4He concentrations leading to 6- and 14-fold decreases in $^4\text{He}/^{232}\text{Th}$ from the 32 to 63 μm size fraction to the $<4 \mu\text{m}$ size fraction (Fig. 3). Most of this decrease occurs between the 32–63 and 16–32 μm fractions.

These grain size effects may be of secondary importance in most distal ocean sediments, where dust is consistently $<20 \mu\text{m}$ and usually $\sim 5 \mu\text{m}$ (Tsoar and Pye, 1987; Rea and Hovan, 1995), as there is only a slight decrease in $^4\text{He}/^{232}\text{Th}$ ratios in grain size fractions $<16 \mu\text{m}$. In these settings, $^4\text{He}/^{232}\text{Th}$ ratios are likely to reflect detrital provenance. Our results suggest that $^4\text{He}/^{232}\text{Th}$ in the fine fraction may differ by a factor of at least two between source areas and may thus be capable of fingerprinting sediment source. We also note that lateral sediment redistribution (“sediment focusing”) is unlikely to impact sedimentary $^4\text{He}/^{232}\text{Th}$ ratios in settings where dust is dominantly fine-grained, as grains $<10 \mu\text{m}$ tend to aggregate in ocean water and are not separated during sediment

resuspension, transport and deposition (McCave and Hall, 2006).

Variations in $^4\text{He}/^{232}\text{Th}$ in size fractions from 16 to 63 μm complicates application of this ratio for estimating dust provenance in proximal sites where dust grain size is relatively coarse and more variable, as variations in $^4\text{He}/^{232}\text{Th}$ between sites and downcore could plausibly represent changes in dust grain size rather than changes in provenance.

5.3.2. Comparison of source area $^4\text{He}/^{232}\text{Th}$ with downwind ocean sediments

$^4\text{He}/^{232}\text{Th}$ ratios in all marine samples are shown in Fig. 7. Ratios are calculated using $^4\text{He}_{\text{TERR}}$ (Eq. (2)). Marine sediment samples from the Pacific Ocean and South Atlantic analyzed or compiled in this study have $^4\text{He}/^{232}\text{Th}$ ratios ranging from ~ 10 to 250 mcc STP/g. Samples immediately downwind of dust source areas have ratios that are generally similar to ratios of fine-grained sediments in their respective source areas (Fig. 7). Mean $^4\text{He}/^{232}\text{Th}$ ratios range from ~ 90 to 180 mcc STP/g in the region of maximum East Asian dust deposition in the North Pacific, similar to the mean $^4\text{He}/^{232}\text{Th}$ ratio of the fine fraction of East Asian source area samples (142 ± 14 mcc STP/g). Values are 187 ± 68 and 202 ± 59 mcc STP/g in Tasman Sea sediments under the Australian dust plume, similar to ratios in Australian source area sediments (209 ± 34 mcc STP/g). In ODP1237 in the southeastern tropical Pacific, which is thought to receive dust from the Atacama and Altiplano regions, $^4\text{He}/^{232}\text{Th}$ ratios average 128 ± 42 mcc STP/g. This value agrees with mean values for Puna-CWA samples (132 ± 30 mcc STP/g), though it should be noted that all Puna-CWA samples come from the eastern side of the

Andes and thus may not be representative of dust reaching ODP1237.

In three cores from the open-ocean South Atlantic ($43\text{--}46^\circ\text{S}$), a region thought to receive primarily South American dust (Li et al., 2008), $^4\text{He}/^{232}\text{Th}$ ratios range from 190 to 250 mcc STP/g. These values are somewhat higher than fine-grained Puna-CWA source area sediments (132 ± 30 mcc STP/g) and much higher than samples from Patagonia (44 ± 10 mcc STP/g). There is no significant difference in $^4\text{He}/^{232}\text{Th}$ ratios between glacial (215 ± 16 mcc STP/g, $n = 6$) and Holocene (250 ± 52 mcc STP/g, $n = 3$) samples in the South Atlantic cores, suggesting consistent detrital provenance through glacial–interglacial cycles. This indication that Patagonian sources may not be significant contributors of dust to the mid-latitude South Atlantic is somewhat surprising, as most prior studies have emphasized Patagonia as the primary source of windblown (Kumar et al., 1995; Martínez-García et al., 2009, 2014) or current-transported (Noble et al., 2012) detrital material to this region and have pointed to glacial outwash from the Patagonian ice sheet as a driver of increases in detrital fluxes to the South Atlantic and Southern Ocean during glacial periods (Sugden et al., 2009; Noble et al., 2012). Though these preliminary results require testing through additional analyses of South American dust sources and South Atlantic sediments, at present they suggest that the Puna-Central West Argentina region of central South America is a more important source of dust to the South Atlantic during both glacial and interglacial periods (Gaiero, 2007).

$^4\text{He}/^{232}\text{Th}$ ratios appear to drop with distance from dust sources, falling to a minimum near the equator in the Pacific Ocean. In the central Pacific, $^4\text{He}/^{232}\text{Th}$ drops from

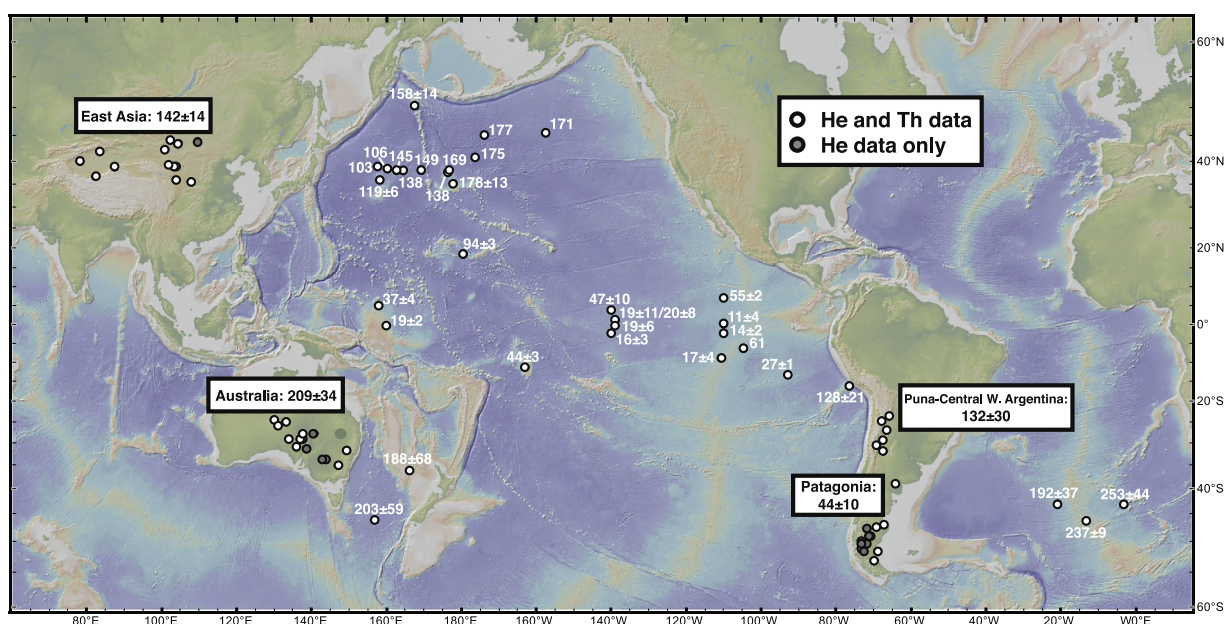


Fig. 7. Map of $^4\text{He}/^{232}\text{Th}$ ratios in samples from this study. All values are expressed in units of mcc STP $^4\text{He}/\text{g } ^{232}\text{Th}$. Average values (± 1 standard error of the mean) are shown for fine fraction (<4 or $<5 \mu\text{m}$) dust source area samples from East Asia, Australia, Puna-Central West Argentina and Patagonia. $^4\text{He}/^{232}\text{Th}$ ratios are shown for each ocean site; where more than one sample was analyzed, the standard error of the mean is also reported.

>120 mcc STP/g north of 20°N to 95 ± 6 mcc STP/g at 18°N to 47 ± 10 mcc STP/g at 4°N to <20 mcc STP/g at sites within 2° north and south of the equator (Figs. 5 and 6). Similarly low ratios are observed in the Paleogene section of ODP Site 1209 with an estimated paleolatitude of 10–15°N (36 ± 2 mcc STP/g) (Marcantonio et al., 2009; Woodard et al., 2012). The causes and implications of low $^4\text{He}/^{232}\text{Th}$ in equatorial Pacific sediments will be explored in the next section.

5.3.3. Significance of low $^4\text{He}/^{232}\text{Th}$ in equatorial Pacific sediments

$^4\text{He}/^{232}\text{Th}$ in sites in the equatorial Pacific appear to be a factor of ~ 10 lower than in midlatitude North and South Pacific sites, and approximately half of this change occurs within 10° of the equator (Fig. 7). As eolian dust flux records based on ^4He and ^{232}Th have been constructed in both Pleistocene and Paleogene low-latitude Pacific sediments (Patterson et al., 1999; Winckler et al., 2005, 2008; Anderson et al., 2006; McGee et al., 2007; Marcantonio et al., 2009; Woodard et al., 2012), it is important to understand this apparent difference in the relationship of ^4He and ^{232}Th between equatorial sediments and sites at higher latitudes. We note that the magnitude of $^4\text{He}/^{232}\text{Th}$ ratios in tropical Pacific sediments is sensitive to the choice of $^3\text{He}/^4\text{He}$ ratio assumed for extraterrestrial He ($^3\text{He}/^4\text{He}_{\text{IDP}}$) in the deconvolution of terrigenous and extraterrestrial ^4He (Section 3.1). The estimates in this paper use a high value for $^3\text{He}/^4\text{He}_{\text{IDP}}$ and thus represent a maximum estimate for tropical $^4\text{He}/^{232}\text{Th}$ ratios; use of a lower value would only increase the magnitude of the drop in $^4\text{He}/^{232}\text{Th}$ ratios from the midlatitudes to the tropics.

A first explanation for the observed decrease in $^4\text{He}/^{232}\text{Th}$ ratios near the equator is a reduction in dust grain size with increasing transport. If dust deposited at the equator were to be finer grained than in regions to the north and south, $^4\text{He}/^{232}\text{Th}$ ratios may be substantially lower at the equator. Grain size separates from East Asian samples suggest a factor of 2–3 decrease in $^4\text{He}/^{232}\text{Th}$ ratios from the 4 to 8 μm fraction to the 0–4 μm fraction, but ratios in the 0–4 μm fractions of East Asian dust (65–220 mcc STP/g) are still substantially higher than observed near the equator (<20 mcc STP/g). It may be that preferential loss of trace phases likely to be enriched in ^4He may also contribute to lower $^4\text{He}/^{232}\text{Th}$ ratios near the equator, similar to inferences based on changing Hf isotope compositions of African dust with increasing distance across the Atlantic Ocean (Aarons et al., 2013; Pourmand et al., 2014). However, the relatively high $^3\text{He}/^4\text{He}$ ratios found in the fine fractions of source area sediments suggest that most He in the fine fraction is not contained in dense, U-rich trace phases like zircon but may instead be in moderate-density phases such as amphiboles and iron oxides and oxyhydroxides (Section 5.1.2).

A second potential explanation for the pattern of falling $^4\text{He}/^{232}\text{Th}$ near the equator is a change in the provenance of detrital material south of the ITCZ from high- $^4\text{He}/^{232}\text{Th}$ Asian and/or North American dust to low- $^4\text{He}/^{232}\text{Th}$ material such as local ocean island volcanics or Central/South American ash. Consistent with a change in provenance,

detrital Nd isotope compositions change significantly along meridional profiles at 140°W and 110°W, going from less radiogenic values similar to East Asian dust at $\sim 5^\circ\text{N}$ to more radiogenic values typical of arc and volcanism south of the equator (Nakai et al., 1993; Ziegler et al., 2008; Xie and Marcantonio, 2012). Along 140°W this pattern, along with concomitant changes in trace element ratios, has been explained by mixing of northern-sourced dust (likely from East Asia) with a combination of volcanic detritus from the Marquesas islands at 10°S, South American ash south of the equator and detrital inputs from the equatorial undercurrent (EUC) immediately at the equator (Ziegler et al., 2008).

To what extent could mixing between East Asian dust and low- $^4\text{He}/^{232}\text{Th}$ volcanic or EUC sediments drive the decrease in $^4\text{He}/^{232}\text{Th}$ ratios near the equator? Assuming mixing of Chinese dust with $^4\text{He}/^{232}\text{Th}$ of 50–100 near the equator with a volcanic endmember with $^4\text{He}/^{232}\text{Th} \sim 0$, ^{232}Th deposited at the equator ($^4\text{He}/^{232}\text{Th} \sim 10$ –20) would be 60–90% from the volcanic endmember. However, Ziegler et al. (2008) find that the andesitic ash and Marquesas volcanics endmembers generally account for <20% of LGM and Holocene detrital sediments at 2°S, the southernmost site at 140°W for which we have $^4\text{He}/^{232}\text{Th}$ data. Detrital sediments from the equatorial undercurrent account for $\sim 30\%$ of detrital sediments within 2° of the equator in their mixing model, but it is likely that this source does not supply significant ^{232}Th , as meridional profiles of ^{232}Th accumulation rates at 140°W and 110°W show a smooth drop from 4–7°N to 2–3°S, with no indication of an equatorial ^{232}Th source (Fig. 8) (Anderson et al., 2006; McGee et al., 2007).

The mixing hypothesis is also difficult to reconcile with the constancy of $^4\text{He}/^{232}\text{Th}$ ratios at equatorial sites across glacial–interglacial cycles despite 2.5-fold changes in ^{232}Th and ^4He fluxes (Anderson et al., 2006; McGee et al., 2007; Winckler et al., 2008). Assuming that volcanic and EUC inputs do not systematically increase during glacial periods, elemental and isotopic ratios that reflect a combination of sources should shift toward the dust endmember during glacial periods, when dust deposition increases. Consistent with this expectation, Ti/Th ratios at site PC72 (0°, 140°W) decrease during glacials, likely due to increased supply of Asian dust with low Ti/Th relative to inputs from the Marquesas with high Ti/Th (Anderson et al., 2006). The fact that high- and low- ^{232}Th flux samples from equatorial Pacific cores show no difference in $^4\text{He}/^{232}\text{Th}$ ratios (Fig. 9; $r = -0.2$, $p > 0.3$) suggests that ^4He and ^{232}Th dominantly reflect a single (presumably eolian) source rather than a mixture of sources.

A third hypothesis for $^4\text{He}/^{232}\text{Th}$ ratio changes near the equator involves the ability of dissolved ^{232}Th to reach sediments by adsorption on sinking particles. Dust deposition is thought to be the primary source of dissolved ^{232}Th in the open ocean (Andersson et al., 1995; Roy-Barman et al., 1996), and so higher dust fluxes north of the ITCZ could produce a meridional gradient in dissolved ^{232}Th concentrations that is proportional to the gradient in dust deposition. Dissolved ^{232}Th transported down gradient could, in theory, be scavenged at low-dust, high-particle flux sites

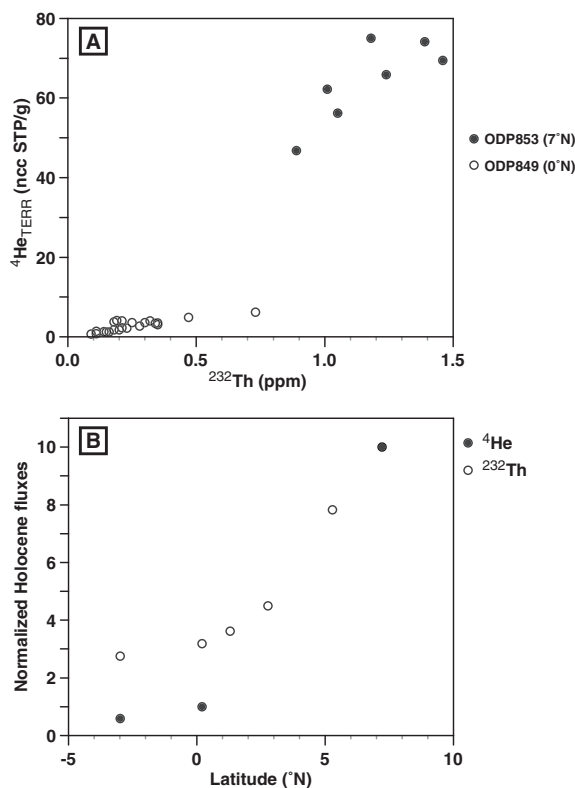


Fig. 8. Comparison of He and Th in tropical Pacific sediments from 110°W. (A) Plot of ${}^4\text{He}_{\text{TERR}}$ vs. ${}^{232}\text{Th}$ concentrations in all samples from two cores along 110°W: ODP853 at 7.2°N, and ODP849 at 0.2°N. The very different slopes of the two arrays make clear the relative depletion of He with respect to Th in equatorial sediments. (B) ${}^{230}\text{Th}$ -normalized ${}^4\text{He}_{\text{TERR}}$ and ${}^{232}\text{Th}$ fluxes from Holocene samples from a meridional transect of cores along 110°W (ODP848–853; McGee et al., 2007; Winckler et al., 2008). Fluxes are arbitrarily normalized such that the flux at ODP853 (7.2°N) is given a value of 10. ${}^{232}\text{Th}$ fluxes fall by a factor of ~ 3.5 from ODP853 to ODP848 (3.0°S), while ${}^4\text{He}_{\text{TERR}}$ fluxes fall by a factor of 17.

near the equator, increasing ${}^{232}\text{Th}$ fluxes there. Helium behaves quite differently, as He lost during dust dissolution is not susceptible to scavenging. Scavenged ${}^{232}\text{Th}$ deposited in sediments thus decreases sedimentary ${}^4\text{He}/{}^{232}\text{Th}$ ratios.

This hypothesis proposes that the ratio of scavenged ${}^{232}\text{Th}$:total ${}^{232}\text{Th}$ increases south of the ITCZ, rising to >0.75 near the equator, based on the observed change in ${}^4\text{He}/{}^{232}\text{Th}$ ratios. Though quantitative evaluation of this hypothesis awaits higher-quality water column Th measurements from the equatorial Pacific, JGOFS data do not show any meridional gradient in water column Th concentrations (Anderson, 2002) inconsistent with this hypothesis. Second, the magnitude of the lateral transport required – enough to make up 75% of sedimentary ${}^{232}\text{Th}$ in equatorial cores – appears incompatible with the short residence time of Th in the upper water column (3–6 years in the upper 500 m; Hayes et al., 2013). Finally, this hypothesis is inconsistent with near-constant Nd/Th ratios between 7°N and 2°S along the 110°W meridional transect (Xie and Marcantonio, 2012); Nd/Th weight ratios average $2.0\text{--}3.0 \times 10^{-3}$ over the last 25 ka in the detrital fraction

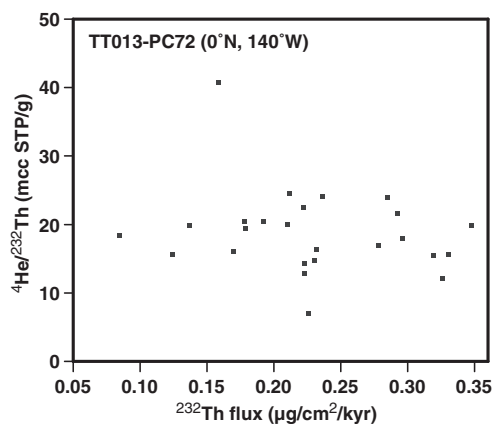


Fig. 9. Plot of ${}^4\text{He}_{\text{TERR}}/{}^{232}\text{Th}$ ratios vs. ${}^{230}\text{Th}$ -normalized ${}^{232}\text{Th}$ fluxes in samples from the equatorial site TT013-PC72 at 140°W (Winckler et al., 2008). There is no significant correlation between the two variables ($r = -0.20$, $p > 0.3$). The lack of change in He/Th ratios with changing Th flux makes it difficult to explain low equatorial He/Th ratios as resulting from mixing, as constant proportions of high-He/Th dust and low-He/Th volcanic material would have to be maintained despite 2.5-fold changes in dust flux.

of all cores. As the residence time of Nd is a factor of ~ 10 greater than that of Th in the open ocean (Bacon and Anderson, 1982; Tachikawa et al., 2003), lateral transport and scavenging of dissolved Nd is not expected to scale with that of dissolved Th. Near-constant ratios are most easily explained by both elements dominantly being hosted within detrital inputs.

We therefore conclude that lateral transport of dissolved ${}^{232}\text{Th}$ from high-dust regions north of the equator followed by scavenging and burial near the equator appears unlikely to explain the data. Decreasing dust grain size south of the ITCZ is perhaps the most likely explanation for a pronounced minimum in ${}^4\text{He}/{}^{232}\text{Th}$ ratios near the equator, but it lacks observational evidence.

6. CONCLUSIONS

${}^{232}\text{Th}$ concentrations are relatively constant in similar grain size fractions from dust source areas in China, Australia and central South America and rise substantially with decreasing grain size. In fine fraction samples (<4 or $<5 \mu\text{m}$) reflecting the approximate grain size of long-traveled eolian dust, concentrations average $14 \pm 1 \mu\text{g}/\text{g}$ in all three source areas. We therefore recommend use of this value in studies using ${}^{232}\text{Th}$ fluxes to estimate dust fluxes in sediments where dust inputs are likely to be fine-grained. This result suggests that studies assuming a ${}^{232}\text{Th}$ concentration of 10–11 $\mu\text{g}/\text{g}$ in eolian dust may overestimate dust fluxes by 30–40% in regions receiving primarily fine-grained dust. ${}^{232}\text{Th}$ concentrations appear to be significantly lower in the fine fraction of Patagonian dust ($\sim 9 \mu\text{g}/\text{g}$) based on our data and previously published results (Gaiero et al., 2004, 2007), suggesting that this lower value should be used in locations receiving exclusively Patagonian dust.

${}^4\text{He}$ concentrations and ${}^3\text{He}/{}^4\text{He}$ ratios are variable in the $<63 \mu\text{m}$ fraction of terrestrial sediments from different source areas, likely due to differences in age, parent element

(U, Th, Li) concentrations, mineralogy, retention of mantle He and grain size. Data from grain size fractions indicate a substantial decrease in ^4He concentrations and increase in $^3\text{He}/^4\text{He}$ with decreasing grain size. High $^3\text{He}/^4\text{He}$ ratios ($>10^{-7}$) in the fine fraction suggest that phases other than zircon, such as iron oxides and oxyhydroxides and possibly amphiboles, are the dominant hosts for He in long-traveled dust. These high ratios also suggest that studies involving $^3\text{He}_{\text{ET}}$ may need to consider higher $^3\text{He}/^4\text{He}$ values for the terrigenous He endmember.

Importantly, ^4He concentrations are quite consistent in the fine fraction of dust source area samples from East Asia, Australia and Puna-Central West Argentina, with mean values in all three regions of $\sim 2 \mu\text{cc STP/g}$. Fine fraction samples from Patagonia suggest a lower mean ^4He concentration of $\sim 0.8 \mu\text{cc STP/g}$. The consistency of these values suggests that ^4He fluxes in distal deposits such as open-ocean sediments and ice cores may be used to offer quantitative dust flux estimates.

Our preliminary survey of marine sediments suggests that $^4\text{He}/^{232}\text{Th}$ ratios in the fine fraction of terrestrial samples are similar to ratios in downwind marine sediments. $^4\text{He}/^{232}\text{Th}$ ratios may thus provide useful provenance information in sites where dust grain size is constrained; one possible application would be in distinguishing Patagonian dust from Puna-Central West Argentina dust and Australian dust in Southern Ocean sediments and Antarctic ice given the much lower $^4\text{He}/^{232}\text{Th}$ ratios in Patagonian source area sediments. Grain size effects on both ^4He and ^{232}Th lead to large decreases in $^4\text{He}/^{232}\text{Th}$ ratios with decreasing grain size, complicating the use of this ratio for provenance investigations in source-proximal sediments with widely varying dust grain size. In the equatorial Pacific, $^4\text{He}/^{232}\text{Th}$ ratios fall by a factor of >4 from $\sim 10^\circ\text{N}$ to the equator. Additional water column Th isotope measurements, measurements of the grain size of lithogenic sediments, and $^4\text{He}/^{232}\text{Th}$ data from modern atmospheric dust in the region may help in determining the reason for this change.

ACKNOWLEDGEMENTS

We thank P. De Deckker and P. Vallenga for providing samples and valuable input and Igor Tolstikhin for helpful discussions. Martin Fleisher, Linda Baker and Roseanne Schwartz provided important assistance and input with sample preparation and analysis. We thank editor Dominik Weiss, Sujoy Mukhopadhyay, Franco Marcantonio and one anonymous reviewer for thoughtful and constructive reviews that improved the manuscript. The Ocean Drilling Program provided samples from ODP Sites 882 and 1208. Partial support for this work was provided by NSF award OCE-1060907 to G.W. and R.F.A. and OREGSU S1315A-D to G.W., a sub-award to NSF award PLR 0968391

APPENDIX A. SUPPLEMENTARY DATA

Supplementary data associated with this article can be found, in the online version, at <http://dx.doi.org/10.1016/j.gca.2015.11.023>.

REFERENCES

- Aarons S. M., Aciego S. M. and Gleason J. D. (2013) Variable Hf–Sr–Nd radiogenic isotopic compositions in a Saharan dust storm over the Atlantic: Implications for dust flux to oceans, ice sheets and the terrestrial biosphere. *Chem. Geol.* **349–350**, 18–26. <http://dx.doi.org/10.1016/j.chemgeo.2013.04.010>.
- Adkins J., deMenocal P. and Eshel G. (2006) The “African humid period” and the record of marine upwelling from excess ^{230}Th in Ocean Drilling Program Hole 658C. *Paleoceanography* **21**. <http://dx.doi.org/10.1029/2005PA001200>.
- Allmendinger R. W., Jordan T. E., Kay S. M. and Isacks B. L. (1997) The evolution of the Altiplano-Puna plateau of the Central Andes. *Annu. Rev. Earth Planet. Sci.* **25**, 139–174.
- Amidon W. H. and Farley K. A. (2011) Cosmogenic ^3He production rates in apatite, zircon and pyroxene inferred from Bonneville flood erosional surfaces. *Quat. Geochronol.* **6**, 10–21.
- Anderson, R. F. (2002). Radionuclides from GoFlo water bottle samples. United States JGOFS Data Server. Woods Hole Oceanographic Institution, USA: U.S. JGOFS Data Management Office, iPub: April 22, 2002. Accessed: November 2, 2009. http://usjgofs.whoi.edu/jg/serv/jgofs/eqpac/tto13/rad_GoFlo.html0.
- Anderson, R. F. (2003). Radionuclides from sediment cores, United States JGOFS Process Study Data 1989–1998. CD-ROM volume 1, version 2, Woods Hole Oceanographic Institution, USA: U.S. JGOFS Data Management Office.
- Anderson R. F. and Fleer A. P. (1982) Determination of natural actinides and plutonium in marine particulate material. *Anal. Chem.* **54**, 1142–1147.
- Anderson R. F., Bacon M. and Brewer P. (1983) Removal of Th-230 and Pa-231 from the open ocean. *Earth Planet. Sci. Lett.* **62**, 7–23.
- Anderson R. F., Fleisher M. Q. and Lao Y. (2006) Glacial–interglacial variability in the delivery of dust to the central equatorial Pacific Ocean. *Earth Planet. Sci. Lett.* **242**, 406–414.
- Andersson P. S., Wasserburg G. J., Chen J. H., Papanastassiou D. A. and Ingri J. (1995) ^{238}U – ^{234}U and ^{232}Th – ^{230}Th in the Baltic sea and in river water. *Earth Planet. Sci. Lett.* **130**, 217–234.
- Andrews J. N. (1985) The isotopic composition of radiogenic helium and its use to study groundwater movement in confined aquifers. *Chem. Geol.* **49**, 339–351.
- Arraes-Mescoff R., Roy-Barman M., Coppola L., Souhaut M., Tachikawa K., Jeandel C., Sempere R. and Yoro C. (2001) The behavior of Al, Mn, Ba, Sr, REE and Th isotopes during in vitro degradation of large marine particles. *Mar. Chem.* **73**, 1–19.
- Bacon M. P. and Anderson R. F. (1982) Distribution of thorium isotopes between dissolved and particulate forms in the deep sea. *J. Geophys. Res.* **87**, 2045–2056.
- Ballentine C. J. and Burnard P. G. (2002) Production, release and transport of noble gases in the continental crust. In *Noble Gases in Geochemistry and Cosmochemistry, Reviews in Mineralogy and Geochemistry* (eds. D. Porcelli, C. J. Ballentine and R. Wieler). Mineralogical Society of America, Washington, D.C.
- Benkert J., Baur H., Signer P. and Wieler R. (1993) He, Ne, and Ar from the solar wind and solar energetic particles in lunar ilmenites and pyroxenes. *J. Geophys. Res.* **98**(13147–13), 162.
- Bettis E., Muhs D., Roberts H. and Wintle A. (2003) Last glacial loess in the conterminous USA. *Quatern. Sci. Rev.* **22**, 1907–1946.
- Biscaye P. E., Grousset F. E., Revel M., Van der Gaast S., Zielinski G. A., Vaars A. and Kukla G. (1997) Asian provenance of glacial dust (stage 2) in the Greenland ice sheet project 2 ice core, summit, Greenland. *J. Geophys. Res.* **102**, 26765–26781.

- Blank M., Leinen M. and Prospero J. M. (1985) Major Asian aeolian inputs indicated by the mineralogy of aerosols and sediments in the western North Pacific. *Nature* **314**, 84–86.
- Bockheim J. G. and Douglass D. C. (2006) Origin and significance of calcium carbonate in soils of southwestern Patagonia. *Geoderma* **136**, 751–762.
- Bradt Miller L. I., Anderson R. F., Fleisher M. Q. and Burckle L. H. (2007) Opal burial in the equatorial Atlantic Ocean over the last 30 ka: implications for glacial–interglacial changes in the ocean silicon cycle. *Paleoceanography* **22**. <http://dx.doi.org/10.1029/2007PA001443>.
- Brook E. J. and Kurz M. D. (1993) Surface-exposure chronology using in situ cosmogenic ^3He in Antarctic quartz sandstone boulders. *Quatern. Res.* **39**, 1–10.
- Brook E. J., Kurz M. D. and Curtice J. (2009) Flux and size fractionation of ^3He in interplanetary dust from Antarctic ice core samples. *Earth Planet. Sci. Lett.* **286**, 565–569.
- Castillo S., Moreno T., Querol X., Alastuey A., Cuevas E., Herrmann L., Mounkaila M. and Gibbons W. (2008) Trace element variation in size-fractionated African desert dusts. *J. Arid Environ.* **72**, 1034–1045.
- Cherniak D. J. and Watson E. B. (2011) Helium diffusion in rutile and titanite, and consideration of the origin and implications of diffusional anisotropy. *Chem. Geol.* **288**, 149–161.
- Claquin T., Roelandt C., Kohfeld K. E., Harrison S. P., Tegen I., Prentice I. C., Balanski Y., Bergametti G., Hansson M., Mahowald N. M., Rodhe H. and Schulz M. (2003) Radiative forcing of climate by ice-age atmospheric dust. *Clim. Dyn.* **20**, 193–202.
- deMenocal P. B., Ortiz J., Guilderson T., Adkins J., Sarnthein M., Baker L. and Yarusinsky M. (2000) Abrupt onset and termination of the African Humid Period: rapid climate responses to gradual insolation forcing. *Q. Sci. Rev.* **19**, 347–361.
- Dubovik O., Holben B., Eck T. F., Smirnov A., Kaufman Y. J., King M. D., Tanre D. and Slutsker I. (2002) Variability of absorption and optical properties of key aerosol types observed in worldwide locations. *J. Atmos. Sci.* **59**, 590–608.
- Farley K. A. (1995) Cenozoic variations in the flux of interplanetary dust recorded by ^3He in a deep-sea sediment. *Nature* **376**, 153–156.
- Farley K. A. (2001) Extraterrestrial helium in seafloor sediments: identification, characteristics and accretion rate over geologic time. In *Accretion of Extraterrestrial Matter Throughout Earth's History* (eds. B. Peucker-Ehrenbrink and B. Schmitz). Kluwer Academic, New York.
- Farley K. A. (2002) (U-Th)/He dating: techniques, calibrations, and applications. *Rev. Mineral. Geochem.* **47**, 819–844.
- Farley K. and Patterson D. (1995) A 100-kyr periodicity in the flux of extraterrestrial He-3 to the sea-floor. *Nature* **378**, 600–603.
- Ferrat M., Weiss D. J., Strekopytov S., Dong S., Chen H., Najorka J., Sun Y., Gupta S., Tada R. and Sinha R. (2011) Improved provenance tracing of Asian dust sources using rare earth elements and selected trace elements for palaeomonsoon studies on the eastern Tibetan Plateau. *Geochim. Cosmochim. Acta* **75**, 6374–6399.
- Fischer H., Siggaard-Andersen M.-L., Ruth U., Rothlisberger R. and Wolff E. (2007) Glacial/interglacial changes in mineral dust and sea-salt records in polar ice cores: sources, transport, and deposition. *Rev. Geophys.* **45**, RG1002.
- Fitzsimmons K. E., Rhodes E. J., Magee J. W. and Barrows T. T. (2007) The timing of linear dune activity in the Strzelecki and Tirari Deserts, Australia. *Quatern. Sci. Rev.* **26**, 2598–2616.
- Fleisher M. Q. and Anderson R. F. (2003) Assessing the collection efficiency of Ross Sea sediment traps using Th-230 and Pa-231. *Deep-Sea Res. Part II* **50**, 693–712.
- Francois R., Frank M., van der Loeff M. and Bacon M. (2004) Th-230 normalization: An essential tool for interpreting sedimentary fluxes during the late Quaternary. *Paleoceanography* **19**, PA1018. <http://dx.doi.org/10.1029/2003PA000939>.
- Frogner P. and Schweda P. (1998) Hornblende dissolution kinetics at 25 °C. *Chem. Geol.* **151**, 169–179.
- Gaiero D. M. (2007) Dust provenance in Antarctic ice during glacial periods: from where in southern South America? *Geophys. Res. Lett.* **34**. <http://dx.doi.org/10.1029/2007GL030520>.
- Gaiero D. M., Brunet F., Probst J.-L. and Depetris P. J. (2007) A uniform isotopic and chemical signature of dust exported from Patagonia: rock sources and occurrence in southern environments. *Chem. Geol.* **238**, 107–120.
- Gaiero D. M., Depetris P. J., Probst J.-L., Bidart S. M. and Leleyter L. (2004) The signature of river- and wind-borne materials exported from Patagonia to the southern latitudes: a view from REEs and implications for paleoclimatic interpretations. *Earth Planet. Sci. Lett.* **219**, 357–376.
- Graham D. W., Jenkins W. J., Schilling J. G., Thompson G., Kurz M. D. and Humphris S. E. (1992) Helium isotope geochemistry of mid-ocean ridge basalts from the South Atlantic. *Earth Planet. Sci. Lett.* **110**, 133–147.
- Grousset F. E. and Biscaye P. E. (2005) Tracing dust sources and transport patterns using Sr, Nd and Pb isotopes. *Chem. Geol.* **222**, 149–167.
- Hayes C. T., Anderson R. F., Fleisher M. Q., Serno S., Winckler G. and Gersonde R. (2013) Quantifying lithogenic inputs to the North Pacific Ocean using the long-lived thorium isotopes. *Earth Planet. Sci. Lett.* **383**, 16–25.
- Hesse P. P. (1994) The record of continental dust from Australia in Tasman Sea sediments. *Quatern. Sci. Rev.* **13**, 257–272.
- Hilton D. R. (1986) *A study of hydrothermal systems using rare gas isotopes* Ph.D. dissertation. University of Cambridge.
- Hsieh Y.-T., Henderson G. M. and Thomas A. L. (2011) Combining seawater ^{232}Th and ^{230}Th concentrations to determine dust fluxes to the surface ocean. *Earth Planet. Sci. Lett.* **312**, 280–290.
- Jahn B. M., Gallet S. and Han J. M. (2001) Geochemistry of the Xining, Xifeng and Jixian sections, Loess Plateau of China: eolian dust provenance and paleosol evolution during the last 140 ka. *Chem. Geol.* **178**, 71–94.
- Jeong G. Y., Hillier S. and Kemp R. A. (2008) Quantitative bulk and single-particle mineralogy of a thick Chinese loess-paleosol section: implications for loess provenance and weathering. *Quatern. Sci. Rev.* **27**, 1271–1287.
- Jickells T. D., An Z. S., Andersen K. K., Baker A. R., Bergametti G., Brooks N., Cao J. J., Boyd P. W., Duce R. A., Hunter K. A., Kawahata H., Kubilay N., laRoche J., Liss P. S., Mahowald N., Prospero J. M., Ridgwell A. J., Tegen I. and Torres R. (2005) Global iron connections between desert dust, ocean biogeochemistry and climate. *Science* **308**, 67–71.
- Jones C. E., Halliday A. N., Rea D. K. and Owen R. M. (2000) Eolian inputs of lead to the North Pacific. *Geochim. Cosmochim. Acta* **64**, 1405–1416.
- Kawahata H. (2002) Shifts in oceanic and atmospheric boundaries in the Tasman Sea (Southwest Pacific) during the Late Pleistocene: evidence from organic carbon and lithogenic fluxes. *Palaeogeogr. Palaeoclimatol. Palaeoecol.* **184**, 225–249.
- Kohfeld K. E. and Harrison S. P. (2003) Glacial-interglacial changes in dust deposition on the Chinese Loess Plateau. *Quatern. Sci. Rev.* **22**, 1859–1878.
- Krogh T. E. (1973) Low-contamination method for hydrothermal decomposition of zircon and extraction of U and Pb for isotopic age determinations. *Geochim. Cosmochim. Acta* **37**, 485–494.

- Kumar N. (1994) *Trace metals and natural radionuclides as tracers of ocean productivity* Ph.D. dissertation. Columbia University.
- Kumar N., Anderson R., Mortlock R., Froelich P., Kubik P., Dittrich-Hannen B. and Suter M. (1995) Increased biological productivity and export production in the glacial Southern Ocean. *Nature* **378**, 675–680.
- Kurz M. D., Curtice J., Lott D. E. and Solow A. (2004) Rapid helium isotopic variability in Mauna Kea shield lavas from the Hawaiian Scientific Drilling Project. *Geochem. Geophys. Geosyst.* **5**. <http://dx.doi.org/10.1029/2002GC000439>.
- Kylander M. E., Muller J., Wust R. A. J., Gallagher K., Garcia-Sanchez R., Coles B. J. and Weiss D. J. (2007) Rare earth element and Pb isotope variations in a 52 kyr peat core from Lynch's Crater (NE Queensland, Australia): proxy development and application to paleoclimate in the Southern Hemisphere. *Geochim. Cosmochim. Acta* **71**, 942–960.
- Lamy F., Gersonde R., Winckler G., Esper O., Jaeschke A., Kuhn G., Ullermann J., Martínez-García A., Lambert F. and Kilian R. (2014) Increased dust deposition in the pacific southern ocean during glacial periods. *Science* **343**, 403–407.
- Leinen M., Cwienk D., Heath G. R., Biscaye P. E., Kolla V., Thiede J. and Dauphin J. P. (1986) Distribution of biogenic silica and quartz in recent deep-sea sediments. *Geology* **14**, 199–203.
- Leinen M., Prospero J. M., Arnold E. and Blank M. (1994) Mineralogy of aeolian dust reaching the North Pacific Ocean: 1. Sampling and Analysis. *J. Geophys. Res.* **99**, 21017–21023.
- Li F., Ginoux P. and Ramaswamy V. (2008) Distribution, transport and deposition of mineral dust in the Southern Ocean and Antarctica: contribution of major sources. *J. Geophys. Res.* **113**. <http://dx.doi.org/10.1029/2007JD009190>.
- Lippolt H. J. and Weigel E. (1988) ^4He diffusion in ^{40}Ar -retentive minerals. *Geochim. Cosmochim. Acta* **52**, 1449–1458.
- Mamyrin B. A. and Tolstikhin I. N. (1984) *Helium Isotopes in Nature*. Elsevier.
- Marcantonio F., Anderson R. F., Stute M., Kumar N., Schlosser P. and Mix A. (1996) Extraterrestrial ^3He as a tracer of marine sediment transport and accumulation. *Nature* **383**, 705–707.
- Marcantonio F., Higgins S., Anderson R. F., Stute M., Schlosser P. and Rasbury E. T. (1998) Terrigenous helium in deep-sea sediments. *Geochim. Cosmochim. Acta* **62**, 1535–1543.
- Marcantonio F., Kumar N., Stute M., Anderson R. F., Seidl M., Schlosser P. and Mix A. (1995) Comparative study of accumulation rates derived by He and Th isotope analysis of marine sediments. *Earth Planet. Sci. Lett.* **133**, 549–555.
- Marcantonio F., Anderson R. F., Higgins S., Fleisher M., Stute M. and Schlosser P. (2001a) Abrupt intensification of the SW Indian Ocean monsoon during the last deglaciation: constraints from Th, Pa and He isotopes. *Earth Planet. Sci. Lett.* **184**, 505–514.
- Marcantonio F., Anderson R. F., Higgins S., Stute M., Schlosser P. and Kubik P. (2001b) Sediment focusing in the central equatorial Pacific Ocean. *Paleoceanography* **16**, 260–267.
- Marcantonio F., Thomas D. J., Woodard S., McGee D. and Winckler G. (2009) Extraterrestrial ^3He in Paleocene sediments from Shatsky Rise: constraints on sedimentation rate variability. *Earth Planet. Sci. Lett.* **287**, 24–30.
- Marchandise S., Robin E., Ayrault S. and Roy-Barman M. (2014) U–Th–REE–Hf bearing phases in Mediterranean Sea sediments: implications for isotope systematics in the ocean. *Geochim. Cosmochim. Acta* **131**, 47–61.
- Martel D. J., Onions R. K., Hilton D. R. and Oxburgh E. R. (1990) The role of element distribution in production and release of radiogenic helium: the Carnmenellis Granite, Southwest England. *Chem. Geol.* **88**, 207–221.
- Martínez-García A., Rosell-Melé A., Geibert W., Gersonde R., Masqué P., Gaspari V. and Barbante C. (2009) Links between iron supply, marine productivity, sea surface temperature and CO_2 over the last 1.1 Ma. *Paleoceanography* **24**, 1–14.
- Martínez-García A., Sigman D. M., Ren H., Anderson R. F., Straub M., Hodell D. A., Jaccard S. L., Eglinton T. I. and Haug G. H. (2014) Iron fertilization of the subantarctic ocean during the last ice age. *Science* **343**, 1347–1350. <http://dx.doi.org/10.1126/science.1246848>.
- Marx S. K., Kamber B. S. and McGowan H. A. (2005a) Estimates of Australian dust flux into New Zealand: quantifying the eastern Australian dust plume pathway using trace element calibrated ^{210}Pb as a monitor. *Earth Planet. Sci. Lett.* **239**, 336–351.
- Marx S. K., Kamber B. S. and McGowan H. A. (2005b) Provenance of long-travelled dust determined with ultra-trace-element composition: a pilot study with samples from New Zealand glaciers. *Earth Surf. Proc. Land.* **30**, 699–716.
- McCave I. N. and Hall I. R. (2006) Size sorting in marine muds: processes, pitfalls, and prospects for paleoflow-speed proxies. *Geochem. Geophys. Geosyst.* **7**, Q10N05.
- McGee D. and Mukhopadhyay S. (2013) Extraterrestrial He in sediments: From recorder of asteroid collisions to timekeeper of global environmental changes. In *The Noble Gases as Geochemical Tracers* (ed. P. Burnard). Springer-Verlag, Berlin, pp. 155–176.
- McGee D., Broecker W. S. and Winckler G. (2010a) Gustiness: the driver of glacial dustiness? *Quatern. Sci. Rev.* **29**, 2340–2350. <http://dx.doi.org/10.1016/j.quascirev.2010.06.009>.
- McGee D., deMenocal P. B., Winckler G., Stuut J. B. W. and Bradtmiller L. I. (2013) The magnitude, timing and abruptness of changes in North African dust deposition over the last 20,000 yr. *Earth Planet. Sci. Lett.* **371–372**, 163–176.
- McGee D., Marcantonio F. and Lynch-Stieglitz J. (2007) Deglacial changes in dust flux in the eastern equatorial Pacific. *Earth Planet. Sci. Lett.* **257**, 215–230.
- McGee D., Marcantonio F., McManus J. F. and Winckler G. (2010b) The response of excess ^{230}Th and extraterrestrial ^3He to sediment redistribution at the Blake Ridge, western North Atlantic. *Earth Planet. Sci. Lett.* **299**, 138–149. <http://dx.doi.org/10.1016/j.epsl.2010.08.029>.
- Merrill J. T., Uematsu M. and Bleck R. (1989) Meteorological analysis of long range transport of mineral aerosols over the North Pacific. *J. Geophys. Res.* **94**, 8584–8598.
- Meyer I., Davies G. R., Vogt C., Kuhlmann H. and Stuut J.-B. W. (2013) Changing rainfall patterns in NW Africa since the Younger Dryas. *Aeolian Res.* **10**, 111–123.
- Miller R. L., Tegen I. and Perlwitz J. (2004) Surface radiative forcing by soil dust aerosols and the hydrologic cycle. *J. Geophys. Res.* **109**. <http://dx.doi.org/10.1029/2003JD004085>.
- Molina-Cruz A. and Price P. (1977) Distribution of opal and quartz on the ocean floor of the subtropical southeastern Pacific. *Geology* **5**, 81–84.
- Morrison P. and Pine J. (1955) Radiogenic origin of helium isotopes in rock. *Ann. N. Y. Acad. Sci.* **62**, 69–92.
- Moore W. S. and Sackett W. M. (1964) Uranium and thorium series inequilibrium in sea water. *J. Geophys. Res.* **69**, 5401–5405.
- Muhs D. R., Budahn J. R., Prospero J. M. and Carey S. N. (2007) Geochemical evidence for African dust inputs to soils of western Atlantic islands: Barbados, the Bahamas and Florida. *J. Geophys. Res.* **112**. <http://dx.doi.org/10.1029/2005JF000445>.
- Mukhopadhyay S. and Farley K. A. (2006) New insights into the carrier phase(s) of extraterrestrial ^3He in geologically old sediments. *Geochim. Cosmochim. Acta* **70**, 5061–5073.

- Mukhopadhyay S. and Kreycik P. (2008) Dust generation and drought patterns in Africa from helium-4 in a modern Cape Verde coral. *Geophys. Res. Lett.* **35**. <http://dx.doi.org/10.1029/2008GL035722>.
- Mussett A. (1969) Diffusion measurements and the potassium-argon method of dating. *Geophys. J. R. Astron. Soc.* **18**, 257–303.
- Nakai S., Halliday A. N. and Rea D. K. (1993) Provenance of dust in the Pacific-ocean. *Earth Planet. Sci. Lett.* **119**, 143–157.
- Nanson G. C., Price D. M., Jones B. G., Maroulis J. C., Coleman M., Bowman H., Cohen T. J., Pietsch T. J. and Larsen J. R. (2008) Alluvial evidence for major climate and flow regime changes during the middle and late Quaternary in eastern central Australia. *Geomorphology* **101**, 109–129.
- Neff J. C., Ballantyne A. P., Farmer G. L., Mahowald N. M., Conroy J. L., Landry C. C., Overpeck J. T., Painter T. H., Lawrence C. R. and Reynolds R. L. (2008) Increasing eolian dust deposition in the western United States linked to human activity. *Nat. Geosci.* **1**, 189–195.
- Nier A. O. and Schlutter D. J. (1992) Extraction of helium from individual interplanetary dust particles by step-heating. *Meteoritics* **27**, 166–173.
- Noble T. L., Piotrowski A. M., Robinson L. F., Mcmanus J. F., Hillenbrand C.-D. and Bory A. J. M. (2012) Greater supply of Patagonian-sourced detritus and transport by the ACC to the Atlantic sector of the Southern Ocean during the last glacial period. *Earth Planet. Sci. Lett.* **317–318**, 374–385.
- Okin G. S., Mahowald N., Chadwick O. A. and Artaxo P. (2004) Impact of desert dust on the biogeochemistry of phosphorus in terrestrial ecosystems. *Global Biogeochem. Cycles* **18**. <http://dx.doi.org/10.1029/2003GB002145>.
- Olivarez A. M., Owen R. M. and Rea D. K. (1991) Geochemistry of eolian dust in Pacific pelagic sediments: implications for paleoclimatic interpretations. *Geochim. Cosmochim. Acta* **55**, 2147–2158.
- Patterson D. B., Farley K. A. and Norman M. D. (1999) ^4He as a tracer of continental dust: A 1.9 million year record of aeolian flux to the west equatorial Pacific Ocean. *Geochim. Cosmochim. Acta* **63**, 615–625.
- Pell S. D., Williams I. S. and Chivas A. R. (1997) The use of protolith zircon-age fingerprints in determining the protosource areas for some Australian dune sands. *Sed. Geol.* **109**, 233–260.
- Pichat S., Abouchami W. and Galer S. J. G. (2014) Lead isotopes in the eastern equatorial Pacific record quaternary migration of the south westerlies. *Earth Planet. Sci. Lett.* **388**, 293–305.
- Pourmand A., Marcantonio F. and Schulz H. (2004) Variations in productivity and eolian fluxes in the northeastern Arabian Sea during the past 110 ka. *Earth Planet. Sci. Lett.* **221**, 39–54.
- Pourmand A., Prospero J. M. and Sharifi A. (2014) Geochemical fingerprinting of trans-Atlantic African dust based on radiogenic Sr–Nd–Hf isotopes and rare earth element anomalies. *Geology* **42**, 675–678.
- Pullen A., Kapp P., McCallister A. T., Chang H., Gehrels G. E., Garzione C. N., Heermance R. V. and Ding L. (2011) Qaidam Basin and northern Tibetan Plateau as dust sources for the Chinese Loess Plateau and paleoclimatic implications. *Geology* **39**, 1031–1034.
- Rea D. K. (1994) The paleoclimatic record provided by eolian deposition in the deep-sea: the geologic history of wind. *Rev. Geophys.* **32**, 159–195.
- Rea D. K. and Hovan S. A. (1995) Grain size distribution and depositional processes of the mineral component of abyssal sediments: lessons from the North Pacific. *Paleoceanography* **10**, 251–258.
- Reiners P. W. and Farley K. A. (1999) Helium diffusion and (U–Th)/He thermochronometry of titanite. *Geochim. Cosmochim. Acta* **68**, 3845–3859.
- Reiners P. W., Spell T. L., Nicolescu S. and Zanetti K. A. (2004) Zircon (U–Th)/He thermochronometry: He diffusion and comparisons with $^{40}\text{Ar}/^{39}\text{Ar}$ dating. *Geochim. Cosmochim. Acta* **68**, 1857–1887.
- Revel-Rolland M., De Deckker P., Delmonte B., Hesse P., Magee J., Basile-Doelsch I., Grousset F. and Bosch D. (2006) Eastern Australia: a possible source of dust in East Antarctica interglacial ice. *Earth Planet. Sci. Lett.* **249**, 1–13.
- Roy-Barman M., Chen J. H. and Wasserburg G. J. (1996) Th-230–Th-232 systematics in the central Pacific Ocean: the sources and the fates of thorium. *Earth Planet. Sci. Lett.* **139**, 351–363.
- Roy-Barman M., Coppola L. and Souhaut M. (2002) Thorium isotopes in the western Mediterranean Sea: an insight into the marine particle dynamics. *Earth Planet. Sci. Lett.* **196**, 161–174.
- Rutherford E. (1905) *Radioactivity*. Cambridge University Press, 580p.
- Saukel C., Lamy F., Stuut J.-B. W., Tiedemann R. and Vogt C. (2011) Distribution and provenance of wind-blown SE Pacific surface sediments. *Mar. Geol.* **280**, 130–142.
- Schroth A. W., Crusius J., Sholkovitz E. R. and Bostick B. C. (2009) Iron solubility driven by speciation in dust sources to the ocean. *Nat. Geosci.* **2**, 337–340.
- Schwertmann U. (1991) Solubility and dissolution of iron-oxides. *Plant Soil* **130**, 1–25.
- Serno S., Winckler G., Anderson R. F., Hayes C. T., McGee D., Machalett B., Ren H., Straub S. M., Gersonde R. and Haug G. H. (2014) Eolian dust input to the Subarctic North Pacific. *Earth Planet. Sci. Lett.* **387**, 252–263.
- Serno S., Winckler G., Anderson R. F., Maier E., Ren H., Gersonde R. and Haug G. H. (2015) Comparing dust flux records from the Subarctic North Pacific and Greenland: implications for atmospheric transport to Greenland and for the application of dust as a chronostratigraphic tool. *Paleoceanography* **30**. <http://dx.doi.org/10.1002/2014PA002748>.
- Sharifi A., Pourmand A., Canuel E. A., Ferer-Tyler E., Peterson L. C., Aichner B., Feakins S. J., Daryaei T., Djamali M., Beni A. N., Lahijani H. A. K. and Swart P. K. (2015) Abrupt climate variability since the last deglaciation based on a high-resolution, multi-proxy peat record from NW Iran: the hand that rocked the Cradle of Civilization? *Quatern. Sci. Rev.* **123**, 215–230.
- Shuster D. L. and Farley K. A. (2005) Diffusion kinetics of proton-induced ^{21}Ne , ^3He and ^4He in quartz. *Geochim. Cosmochim. Acta* **69**, 2349–2359.
- Shuster D. L., Vasconcelos P. M., Heim J. A. and Farley K. A. (2005) Weathering geochronology by (U–Th)/He dating of goethite. *Geochim. Cosmochim. Acta* **69**, 659–673.
- Sokolik I. N. and Toon O. B. (1999) Incorporation of mineralogical composition into models of the radiative properties of mineral aerosol from UV to IR wavelengths. *J. Geophys. Res.* **104**, 9423–9444.
- Solomon D. K., Hunt A. and Poreda R. J. (1996) Source of radiogenic helium 4 in shallow aquifers: implications for dating young groundwater. *Water Resour. Res.* **32**, 1805–1813.
- Stancin A. M., Gleason J. D., Rea D. K., Owen R. M., Moore T. C., Blum J. D. and Hovan S. A. (2006) Radiogenic isotopic mapping of late Cenozoic eolian and hemipelagic sediment distribution in the east-central Pacific. *Earth Planet. Sci. Lett.* **248**, 840–850.
- Sugden D. E., McCulloch R. D., Bory A. J.-M. and Hein A. S. (2009) Influence of Patagonian glaciers on Antarctic dust deposition during the last glacial period. *Nat. Geosci.* **2**, 281–285.
- Sun Y., Chen H., Tada R., Weiss D., Lin M., Toyoda S., Yan Y. and Isozaki Y. (2013) ESR signal intensity and crystallinity of quartz from Gobi and sandy deserts in East Asia and

- implication for tracing Asian dust provenance. *Geochim. Geophys. Geosyst.* **14**. <http://dx.doi.org/10.1002/ggge.20162>.
- Sun Y. B. and An Z. S. (2005) Late Pliocene-Pleistocene changes in mass accumulation rates of eolian deposits on the central Chinese Loess Plateau. *J. Geophys. Res.* **110**, D23101.
- Tachikawa K., Athias V. and Jeandel C. (2003) Neodymium budget in the modern ocean and paleo-oceanographic implications. *J. Geophys. Res. -Oceans* **108**, 13.
- Taylor S. R. and McLennan S. M. (1985) *The Continental Crust: Its Composition and Evolution*. Blackwell Scientific, Oxford.
- Tolstikhin I., Lehmann B. E., Loosli H. H. and Gautschi A. (1996) Helium and argon isotopes in rocks, minerals and related groundwaters: a case study in northern Switzerland. *Geochim. Cosmochim. Acta* **60**, 1497–1514.
- Trull T. W., Kurz M. D. and Jenkins W. J. (1991) Diffusion of cosmogenic ^3He in olivine and quartz; implications for surface exposure dating. *Earth Planet. Sci. Lett.* **103**, 241–256.
- Tsoar H. and Pye K. (1987) Dust transport and the question of desert loess formation. *Sedimentology* **34**, 139–153.
- Vallelonga P., Gabrielli P., Balliana E., Wegner A., Delmonte B., Turetta C., Burton G., Vanhaecke F., Rosman K. J. R., Hong S., Boutron C. F., Cescon P. and Barbante C. (2010) Lead isotopic compositions in the EPICA Dome C ice core and Southern Hemisphere Potential Source Areas. *Quatern. Sci. Rev.* **29**, 247–255.
- Weber E. T., Owen R. M., Dickens G. R., Halliday A. N., Jones C. E. and Rea D. K. (1996) Quantitative resolution of eolian continental crustal material and volcanic detritus in North Pacific surface sediment. *Paleoceanography* **11**, 115–127.
- Weiss D., Shotyk W., Rieley J., Page S., Gloor M., Reese S. and Martinez-Cortizas A. (2002) The geochemistry of major and selected trace elements in a forested peat bog, Kalimantan, SE Asia, and its implications for past atmospheric dust deposition. *Geochim. Cosmochim. Acta* **66**, 2307–2323.
- Wiens R. C., Bochsler P., Burnett D. S. and Wimmer-Schweingruber R. F. (2004) Solar and solar-wind isotopic compositions. *Earth Planet. Sci. Lett.* **222**, 697–712.
- Winckler G. and Fischer H. (2006) 30,000 years of cosmic dust in Antarctic ice. *Science* **313**, 491–491.
- Winckler G., Anderson R. F., Fleisher M. Q., McGee D. and Mahowald N. (2008) Covariant glacial–interglacial dust fluxes in the equatorial Pacific and Antarctica. *Science* **320**, 93–96.
- Winckler G., Anderson R. F. and Schlosser P. (2005) Equatorial Pacific productivity and dust flux during the mid-Pleistocene climate transition. *Paleoceanography* **20**. <http://dx.doi.org/10.1029/2005PA001177>.
- Woodard S. C., Thomas D. J. and Marcantonio F. (2012) Thorium-derived dust fluxes to the tropical Pacific Ocean, 58 Ma. *Geochim. Cosmochim. Acta* **87**, 194–209. <http://dx.doi.org/10.1016/j.gca.2012.03.035>.
- Xie R. C. and Marcantonio F. (2012) Deglacial dust provenance changes in the Eastern Equatorial Pacific and implications for ITCZ movement. *Earth Planet. Sci. Lett.* **317–318**, 386–395.
- Yancheva G., Nowaczyk N., Mingram J., Dulski P., Schettler G., Negendank J., Liu J., Sigman D., Peterson L. and Haug G. (2007) Influence of the intertropical convergence zone on the East Asian monsoon. *Nature* **445**, 74–77.
- Ziegler C. L., Murray R. W., Plank T. and Hemming S. R. (2008) Sources of Fe to the equatorial Pacific Ocean from the Holocene to Miocene. *Earth Planet. Sci. Lett.* **270**, 258–270.

Associate editor: Dominik Weiss